UNIVERSITÀ DEGLI STUDI DI PADOVA

SCUOLA DI SCIENZE
Dipartimento di Geoscienze
Direttore Prof. Nicola Surian

Tesi di laurea magistrale in Geologia Ambientale e Dinamica della Terra LM-74
Curriculum Earth Dynamics

HOW SATELLITES CAN ENRICH RIVER GEOMORPHIC CHARACTERIZATION

Relatore:
Prof. Simone Bizzi
Correlatori:
Ing. Elisa Bozzolan
Dott. Andrea Brenna

Laureanda:
Camilla Vidi

Anno Accademico: 2022-2023

A mio papà, che mi ha permesso di dedicare
tempo, denaro ed energie allo studio di ciò che mi piace,
nonostante le avversità degli ultimi anni.

Ai miei amici, vicini e lontani, con i quali ho condiviso questa esperienza
e mi hanno supportata e sopportata per cinque lunghi anni.

INDEX

List of figures

List of Tables

Abstract

Satellite images-derived data can change the way geomorphology describes patterns and processes of extremely dynamic systems such as rivers. This study focuses on how Sentinel-2 image data can be implemented in traditional classification, to obtain new hints on fluvial dynamics of Po River, in northern Italy.

A traditional classification of the River has been performed, based on orthophotos with centimetric resolution, collected in 2020. The classification for Po River has been done following the guidelines of IDRAIM handbook, and calculating three fundamental indexes: anabranching, braiding and sinuosity, for the distinction of morphological characteristics. Secondly the normalized drainage area (W*) and slope has been calculated. The subdivision of Po River into fundamental units called reaches, and the identification of the most representative of them has been performed.

For each reach identified, Sentinel-2 images, with a maximum resolution of 10 meters, has been downloaded for the period between January 2018 to December 2022. On those, a fuzzy classification has been performed, assigning to each pixel a percentage value of membership to one of the three semantic classes analyzed, which are: water, sediment and vegetation.

The results of traditional classification have been interesting, showing distinctive features of each river morphology defined. W* has shown to be able to distinguish among different morphology even if it was not used in their definition, proving its value as river attribute and its functional links with other river morphological features. Transitional and anabranching patterns are easily distinguishable from straight, sinuous and meandering, due to their high sediment content (considering the same drained area). On the other hand sinuosity, braiding and anabranching indexes are able to distinguish among all the morphologies.

From Sentinel-2 classification more specific trend emerged, that highlight a general decrease of water throughout the 5 years analyzed, and more specific seasonal trends,

pretty evident for vegetation. Moreover has been possible to see the vegetation recover time after a flood event verified in December 2019. Riparian vegetation restore the habitat at the end of summer season, with a strong grew around August-September. For this classification the comparison between water and sediment is very representative of the morphology. Anabranching and transitional reaches are characterized by high amount of sediment and less water, that corresponds with a higher distribution of exposed sediment considered as a morphological unit. Therefore the process that leads to such a distribution is different from the one that creates a single channel, with few exposed sediment, characteristic of straight, meandering and sinuous patterns. A further consideration can be linked with the anthropization of the area, fostering riverbed mining in the past, and channel confinement nowadays, creates an almost sharp distinction between single-channel and multiple-channels morphologies.

The results of the two classifications helped for a deeper understanding of the system. On one hand traditional classifications provide accurate information on the morphology, allowing to have centimetric resolutions. On the other hand satellite-image classification helps with the understanding of the processes that occur in a river system, thanks to their temporal resolution.

Both classifications provide valuable information, that allow a deep understanding of the system, and may help with the creation of models that will try to predict future trends.

1. Introduction

The aim of this thesis is to compare satellite images derived data, with a more traditional characterization of rivers, analysing how the two methods can implement our knowledge of a constantly developing environment, such as rivers.

Since the first aerial photos acquisitions, in 1858, remote sensing technology evolved pretty fast. The availability of remote sensing data became more and more widespread and nowadays have a key role in the understanding of Earth's processes and interactions. Today it is providing its best contribution to the big data era, giving the chance to help governments being more efficient, to improve decision making, product innovation, and are employed in many other different sectors (Chi et al., 2016).

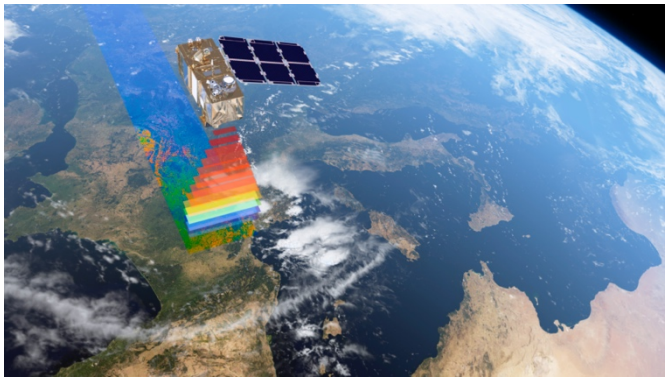

Fig. 1. Color Vision for Copernicus*, 2015. Image credit: ESA Earth Online.*

To what specifically concerns fluvial geomorphology, remote sensing is transforming the way researches are done, starting from mapping, to measuring and analysing data (Marcus & Fonstad, 2010). In fact, one of the main advantages of this technology is related to the acquisition of satellite images, that can occur at predictable time intervals, (Carbonneau & Piegay, 2012) and are the most efficient way to obtain information from huge areas in a short period of time, for example from a river system (Gilvear & Bryant, 2016). Despite this, most of the remote sensing application has been used to validate or test already existing concepts of fluvial geomorphology, instead of creating new ones (Piégay et al., 2020). When implemented they have always been joined by more traditionally acquired data, such as: field surveys, aerial photography, topography or historical mapping (e.g., Boothroyd et al., 2021).

Considering said the above, a fundamental problem exists, and is related to how can we gain new knowledge from big data. On one side there is the opportunity to obtain many data in a very short time, on the opposite side is still a problem to properly exploit them because of their huge complexity and heterogeneity, still with high potential (Ramapriyan, 2013).

The content of this thesis is to compare a traditional classification of rivers, performed on Po River, in northern Italy, with a modern classification based on Sentinel 2 images data acquisition and analysis.

The traditional classification is based on orthophotos taken once every 5 or 10 years. These images are characterised by centimetric resolution, and portrait the situation of a river in the moment of the acquisition. It is a valid method to assess river morphology and conditions and gives the chance to make comparisons between different years. The traditional classification performed in this study case is based on the IDRAIM manual book (Rinaldi et al., 2014). It is constituted by a first assessment phase where three important indexes are defined: sinuosity, anabranching and braiding. On the base of those, and of observable characteristics (dams, confluences…) the subdivision of the river in reaches is performed. The aim of this classification is to define geomorphologically homogeneous parts of the river, in order to understand its behaviour and to apply the best management possible based on its characteristics.

The problem with this type of analysis is that there is a lack in temporal continuity (an image every few years or more), therefore is impossible to properly understand fluctuations and variations in river morphologies through few years and within a year or just after a significant event.

On the other hand, satellite image classifications have the capability to cover a wider temporal range at the expense of spatial resolution that, instead of being of some centimetres, it is minimum of 10 meters. For big river systems is crucial to continuously monitor morphological conditions, because they are very dynamic systems, and can affect huge areas and the population that lives on it. Going into more detail, with these

new methods is possible to investigate the variations in time of water, sediment, and vegetation for each reach. What has been performed in the frame of this thesis is based on the fuzzy classification created by Carbonneau et al. (2020) on Sentinel 2 images. The classification assigns to each pixel a percentage value of belonging to a class. The classes considered are three: one for water, one for sediment and the last for vegetation. The output of all the classification is a NETCDF file that allows to see variations in the values of each pixel through a period of time. The data are than reworked again to obtain graphs that show the changes of the three classes through time.

Po River is the longest river of Italy and is characterised by a good diversity of river patterns. This gives the chance to find a wide range of river morphology that can be analysed with traditional and a satellite-based data; it is the perfect training area to test the reliability of this new tool.

In addition to this, Po River is important for Italy both from an economic and ecological point of view. Moreover, recent (May 2023) floodings occurred in the area, led to a huge devastation of towns and cropland, creating many millions of euros of damages.

In this sense is crucial to create and provide reliable tools that will help administrations in important decision making. The aim, of all the studies on geomorphological evolutions of Po River, is to avoid the implementation of works that aren't based on a profound knowledge of the processes they will affect. This new perspective will try to avoid past errors that has been done in the last 200 years of interventions on the river.

Remote sensing affords considerable potential to not only foster significant advances in our scientific understanding of river systems but also facilitate monitoring and management of these crucial resources (Carbonneau & Piegay, 2012).

The final aim of this study is to understand how satellite images, can enrich traditional geomorphological classification. The idea is to try to verify which new processes can we observe, by considering data that are taken almost continuously in time but have a 10 metres spatial resolution, instead of looking at datasets with a lower temporal resolution (5-10 years), but higher spatial resolution (centimetres).

2. Study area

2.1 Hydrogeographical and geomorphological setting

Po River flows through the Northern part of Italy and is the longest river of this Nation. The headwaters of Po River are located in the Cottian Alps, (close to the border between Italy and France), where the crystalline waters seep down from Pian del Re, a big natural amphitheatre at 2,020 m, under the northwest face of Monviso. The watercourse extends along the 45th parallel and crosses Italy from east to west, creating a clear boundary, used as separating border between Lombardy, Veneto, and Emilia-Romagna. After 651 km of flow, it reaches the Adriatic Sea where it creates the delta coastline, which stretches approximately form the Adige River mouth to 80 km south at the mouth of Goro branch and ends its course.

Po River has the widest drainage area (70,091 km^2), and a mean annual discharge of approximately 1500 m^3s^{-1} (Parrinello et al., 2021). It drains most of North Italy, with a

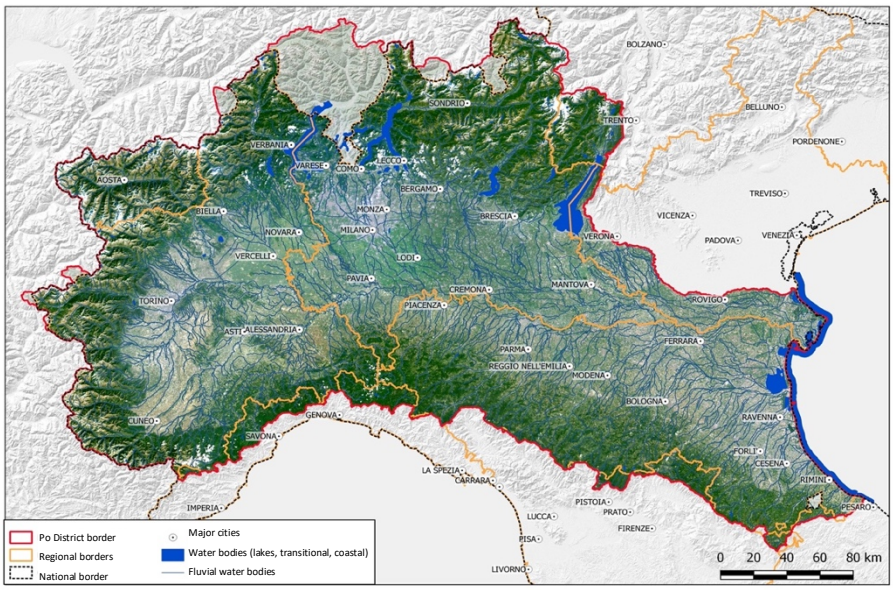

Fig. 2. *Po River District. (AdbPo, 2018)*

catchment that comprehends 141 main tributaries and about 450 lakes. It has an

important role in the drainage of Italy's Alpine rivers, and subalpine lakes such as Lake Garda, Como, and Maggiore. It also drains a large part of the northern Apennines.

The related river network is of about 6750 km and 31 000 km long, for natural and artificial channels, respectively (Montanari, 2012). For these reasons, the Po River is characterised by a complex hydrological network, that collects water from most of northern Italy and its mountains.

This variability results, in practical terms, in a change of the geomorphological characteristics of the reaches. The fact that, in a single river, geomorphological features changes so much, gives to the Po River the perfect attributes to be the best fitting study site.

2.2 Importance of Po River for Italy

The vast valley around the river is called the Po Basin and is the largest alluvial plain in Italy. It's one of the most intensively populated, cultivated and developed areas of Italy and in general of Europe, and more than 40 percent of the entire Italian GDP is produced in its factories and farms (Parrinello, 2018). This alluvial plain has been inhabited for a long time, certainly from prehistory, even if the first written records date back to the late Roman Republic. Starting from the middle age, the lands surrounding the river has been intensively cultivated, and from that time on, the Po basin has become the main agricultural area in Italy.

Fig. 3. *Population density in Italy. Some of the highest values are registered in the Po Plain (ISTAT, 2019).*

Nowadays about 20 million people (demographic density is of about 225 inhabitants per km^2) live in this area, that comprehends among the others, cities such as Turin, Milan, Piacenza, Cremona and Ferrara (Bocchino et al., 2023).

2.3 Anthropic interventions and their effects on river morphology

2.3.1 Anthropic interventions

As presented by Parrinello et al. (2021) anthropic alterations of sediment fluxes are one of the most conspicuous signs of human impact on natural processes, and Po Plain hasn't been spared. Three main processes have changed the geomorphology of the Po River: hydropower production, sand and gravel mining from riverbeds, and extraction of methane gas. For what concerns the aim of this thesis methane extraction is less relevant than the other two processes, so it will not be taken into consideration.

Human pressures on the Po River have a long history, but the first important interventions occurred starting from the nineteenth century. When all Europe implemented coal, Italy, die to the lack of it, had to implement hydroelectrical power stations to grow its industrial sector. Around 1900 Po Palin was invaded by waterwheels, and on Po tributaries started the construction of the first dams (Parrinello, 2018). The important boom occurred after the World War I when industries were driven by hydroelectricity. By the end of 1950s, 142 dams were altering almost every tributary of the Po River. With the construction of the first dam a new problem emerged, in fact dams were trapping water, as well as sediments, which turned out to be the cause of a diminution of construction's efficiency, reducing the space for water.
The issue with dams' construction is actual also nowadays, and can lead to many problems, in fact in some cases, the amount of sediment stolen from the river system is so great that is able to alter the morphology of the river channel, causing incision.

The second problem affecting the Po River, was linked with the mining of riverbed to extract sand and gravels. To have efficient dams the least sediment needs to be present,

and for this reason reforestation programs started. Moreover sand mining became a business because sediments are a fundamental component for modern construction industry (Parrinello et al., 2021). Extractions continued uncontrolled until 1980, when the administrations had to face the problem: whenever an intense flood occurred in a very exploited area, infrastructures were damaged or destroyed, and in the worst scenario people died.

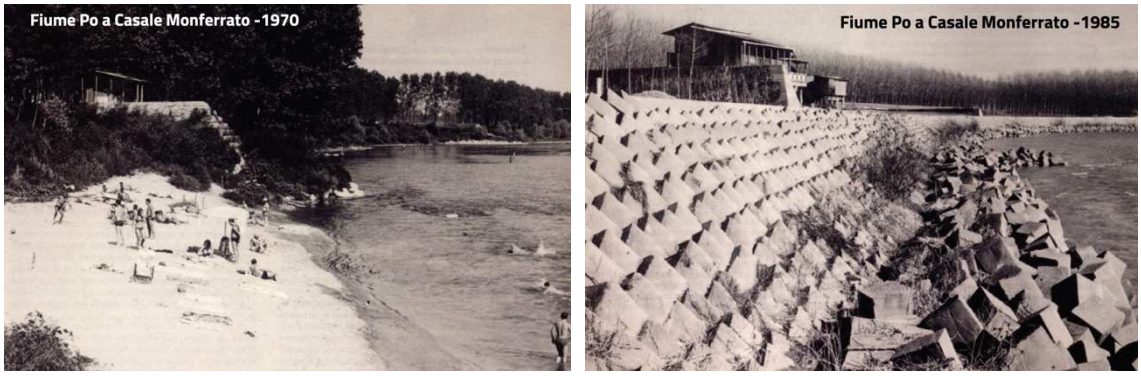

Fig. 4. On the right Po River in Casale Monferrato in 1970, on the left Po river in the same area in 1985, due to sand mining (AdbPo, 2008).

In the end anthropogenic pressure on Po river can be resumed by two main points:

1. Use of territory for residential and economic purposes.
2. Use of water resources, for domestic and industrial supply, irrigation, waste disposal and flood control.

The direct consequence of the relation between the river system and land use is the containment of the river itself, to reclaim areas for croplands, residential and manufacturing activities (*River Restoration in Europe*, 2001).

The complex history of this river, and the infinite number of interventions that it has gone through, create a very complex and compromised system.

Because of its length and geomorphological variations, driven for a strong part by anthropic interventions, Po River is the perfect candidate for renaturation programs.

Within this framework, in 2021 the "Renaturation of the Po area" project has been proposed (AdbPo, 2022). It is one of the most important restoring plans of rivers in Italy and falls under the National Recovery and Resilience Plan (PNRR) founds. Is an

investment covering the entire river course, from it a great impact is expected for the improvement of the river ecosystem, safety and quality of life, for those who live in the areas and tourists.

The project, signed in 2021, pursues the objective of reducing the artificiality of the riverbed, an issue closely linked to the European Strategy for biodiversity to 2030 (AdbPo, 2008; Andrea Colombo, 2022)

The final aim is to produce a more natural river, but still to be able to manage it, trying to do it in a more sustainable and efficient way. The project focuses mainly the middle part of Po River, where 37 areas to re-naturalize have been identified, as well as 7 areas on the Po River Delta. The duration of the financing from the NRRP is from 2021 to 2026, but the aim is to gain other moneys in order to extend the interventions and monitoring part for several more years.

In light of what has been seen so far, the discussion of this thesis can be very useful.

Is crucial to portrait the actual situation and, most of all, the processes that are going on right now, to be able to see future changes.

Therefore the characterization of river morphology is fundamental: more information are gained more is easy to understand which processes are occurring. The consequent step is to verify the effectiveness of renaturation projects, and this can be certainly done by the implementation of new techniques such as satellite image analysis, that can be one of the best time-cost effective solution to adopt.

2.3.2 Consequences on river morphology and monitoring technologies

Fluvial dynamic morphologies and processes are often considered as sources of potential risks for humans and their activities. Bank erosion and the widening of a channel are threats to houses and activities, and the deposition of gravels and sands in the riverbed are perceived as obstacles that clog the river flow. To overcome these potential threatens interventions such as “riverbed cleaning” or the creation of regular riverbed sections are done, not caring about the river morphology and its habitats.

Within this frame, satellite image classifications can be the perfect solutions for a cost-effective management and monitor of the situation, and therefore the application and evaluation of these new tools is a priority.

Moreover the study that is presented here, can be the beginning of a new methodology, that might give the chance to deal with actual changes and understand future trends.

In an evolving planet, due to climate change, being able to predict future trends of river geomorphology can be the only possibility we have to prevent disasters.

Po River is a hybrid creation of nature and humans and is in continuous evolution.

What we have seen until now are the causes that are leading to many morphological changes, such as channel incision, reduction of morphological complexity and channel narrowing (Montanari, 2012).

By a study conducted by (Surian & Rinaldi, 2003), in response to human interventions, Po River, such as many other rivers in Italy, have experienced dramatic adjustment and changes. Usually the modification trends are more intense immediately after the disturbance, than they slowly adjust. Mostly at the beginning they represent a big

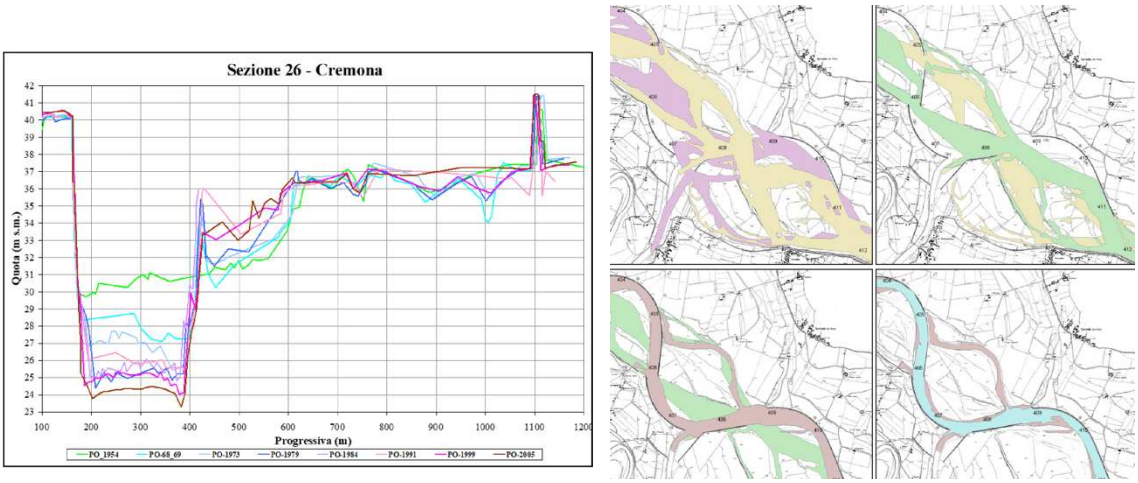

Fig. 5. *On the left: riverbed incision of the section 26- Cremona of Po River, from 1954 until 2005. On the right: narrowing of channel riverbed. Pink 1931, yellow 1953, green 1967, red 1988, light blue 2003* (Andrea Colombo, 2022).

problem because can undermine infrastructures, create loss of groundwater storage and of habitat diversity (Bravard et al., 1999).
In Po River two main incision phases can be recognized. The first starting around the end of XIX sec. and can be linked with the implementation of watermills. The latter started around 1950-1960 and has been due to the start of sediment mining.

In a study done by Surian and Rinaldi (2003)has been described the adjustment of three channel morphologies:

(A) Single thread, that includes both straight and meandering patterns;
(B) Transitional, that includes sinuous with alternate bars and meandering (see chapter 3.1.4);
(C) Braided morphologies, which are characterized by a network of channels separated by ephemeral bars.

Different adjustment take place depending on the degree of incision and narrowing, but in general this phenomenon causes the lowering of the bottom depths, the riverbed sections narrowing and sometimes the variation of the planimetric shape with the transition from dynamic morphologies (intertwined channels) towards more simplified ones (Fig. 6). The effects of this simplification propagate from riverbed to the adjacent fluvial region, creating a wider range of impacts and ecological alterations. However is important to point out that the final result of this scheme doesn't correspond with the last stage of channel evolution (Surian & Rinaldi, 2003). Rivers are one of the most dynamic system in the world, so they will continue to adapt to new situations, driven by humans but also by climate conditions.

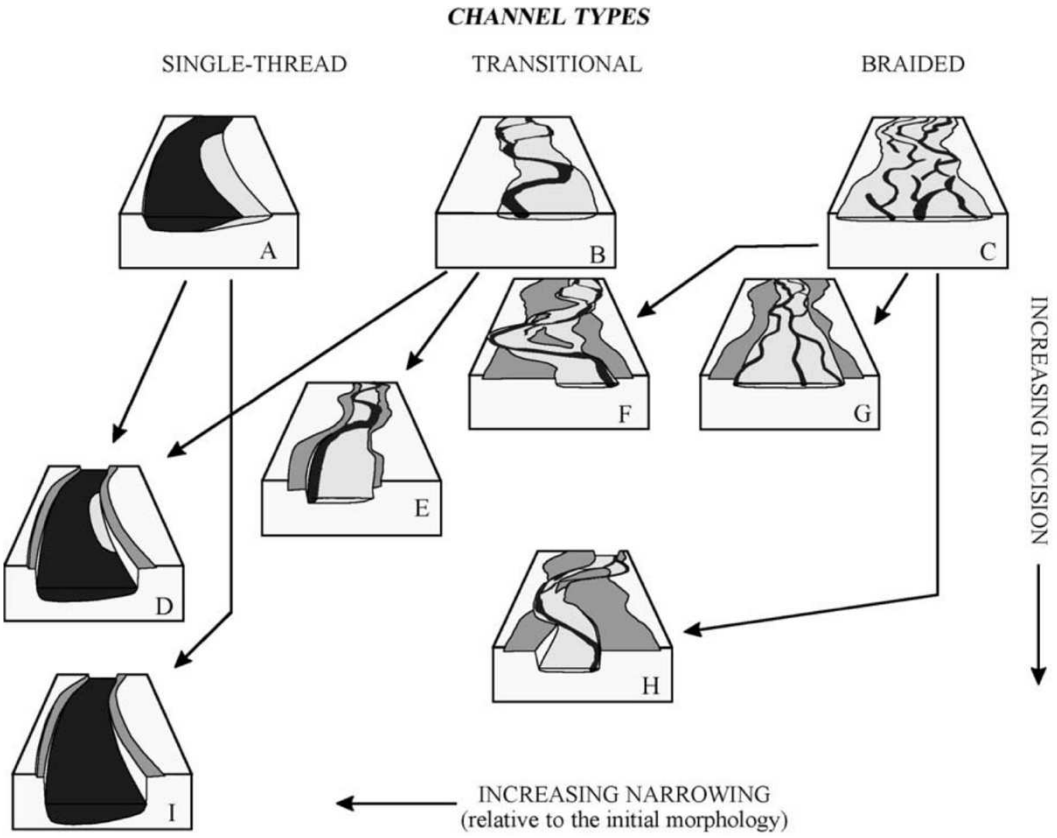

Fig. 6. *Visual explanation of the adjustment made by different river morphologies subjected to channel incision and narrowing (Surian & Rinaldi, 2003).*

Within this frame the aim of this manuscript can help to monitor future fluvial trajectories, and the effectiveness of planned restoration projects. Because the temporal resolution, in this case, will be for sure the most important value to properly estimate a modification in the riverine system.

3. Methods and data

3.1 Traditional classification

3.1.1 IDRAIM

Classification and characterization of river morphology and hydrology are considered to be the baseline for interdisciplinary studies, to understand the behavior and to support river management (Rinaldi et al., 2016).

The methods utilized are linked to the traditional way to classify a river, based on its visible characteristics, seen at the time of the classification. The result of this sorting is a portrait if the situation in a specific moment.

The traditional method used to classify river morphology, in this thesis, is based on the System for stream hydromorphological assessment, analysis, and monitoring.
The handbook IDRAIM constitutes a methodological framework of analysis, post-monitoring evaluations and for the design and implementation of the program of restoration and mitigation measures envisaged by WFD and the Flood Directive 2007/60/CE. The manual's aims are environmental quality and mitigation of flood risks, and therefore it is a helpful tool for the management and support of river courses and geomorphological processes. The IDRAIM project was born in 2008, due to the need of ISPRA to have a systematic procedure and structure to address geomorphological aspect, inserting them into a hydraulic and ecological framework, to build an efficient management of water courses. The framework provides specific consideration of the temporal context, both in terms of reconstructing the trajectory of past channel evolution and to interpret present river conditions and future trends.

The monitoring of morphological parameters and indicators, and the assessment of future scenarios of channel evolution, are fundamental tools created to help the

management of water resources, enhancing morphological quality and/or risk mitigation (ISPRA, 2016).

The IDRAIM toolbox is characterized by four phases:

1. Characterization of the fluvial system: the hydrographic network is subdivided spatially, following a hierarchy for the definition of spatial units.

   To sum up the procedure:

   - Step 1: the catchment is divided into physiographic units, and the river network into segments (macro-reaches);
   - Step 2: streams are characterized based on their lateral confinement;
   - Step 3: the identification and classification of morphological typologies is performed, based on the stream planimetric characteristics.
   - Step 4: additional elements are takin into consideration, such as hydrology, bed slope, sediment, geomorphic units' assemblages, to subdivide the river into homogeneous reaches (reaches are the main scale units for IDRAIM, but further subdivision exists).

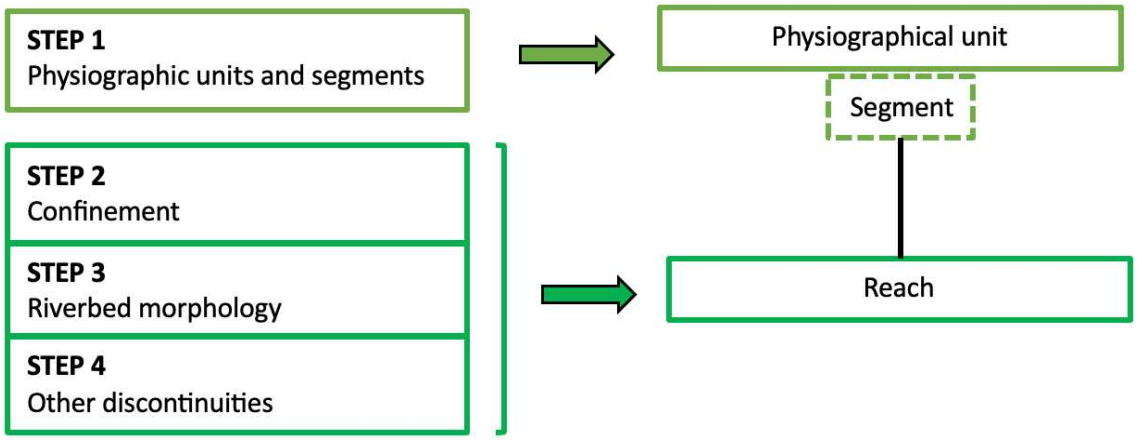

Fig. 7. *Subdivision of the characterization of the fluvial system in steps.*

2. Analysis of past evolution and assessment of current river conditions: in this phase are analyzed temporal changes, in particular past evolutionary trajectories to provide and actual conditions of rivers.

   The second phase analyzes temporal changes to give and evaluation of current river conditions.

3. Future trends: in this phase potential future trajectories of channel morphology are considered. This phase is constituted by two steps:
   - Monitoring, with a periodic measurement of morphological indicators;
   - Modeling, with prediction of future scenarios.

4. Management: the knowledge acquired during the previous steps are used to help decision-makers. An example of a general decision-making framework is shown in Fig. 8.

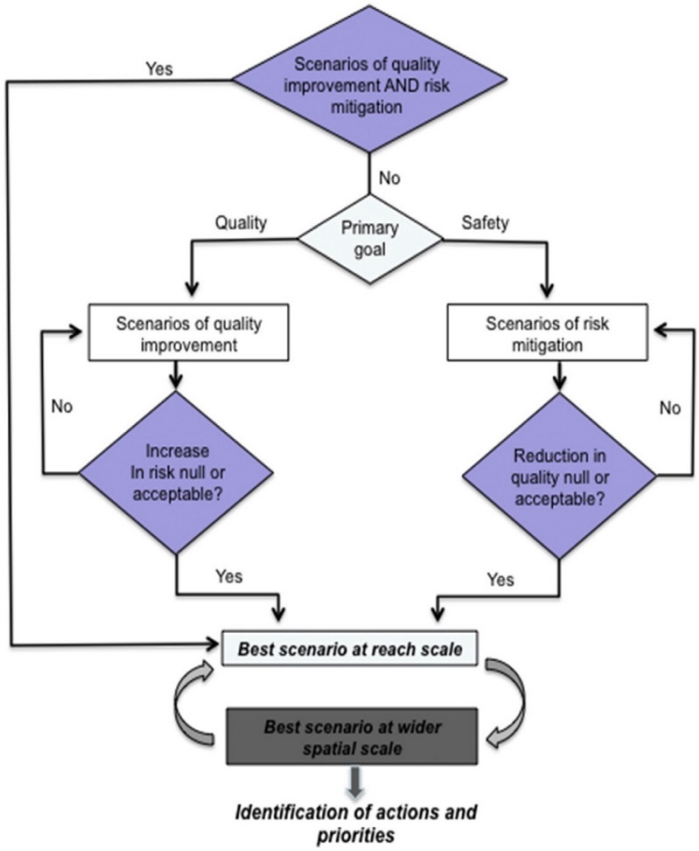

Fig. 8. *General decision-making framework.*

Once the problems are assessed a series of possible intervention scenarios can be provided. The first scenario is to identify a solution that can both increase morphological quality as well as mitigate risks. if this, which would be the best solution, is unapplicable, alternative scenarios are proposed taking into consideration the primary goal problem to be solved. In the following phase the effects of the scenario chosen are

evaluated and actions which minimize adverse effects are highlighted, in order to achieve the best scenario at a reach scale. Afterward a supplementary consideration has to be done, having a look at the effect of the potential intervention at a wider spatial scale (Rinaldi et al., 2014, 2015).

3.1.2 How to analyze a river: necessary steps

The aim of this thesis is to understand how satellite-derived data can enrich the geomorphological knowledge and characterization of rivers.

In order to assess this is therefore fundamental to perform a traditional characterization. The IDRAIM toolbox constitutes the perfect framework to methodologically analyse rivers, and to build a complete traditional classification.

In order to perform a proper classification four steps are required. The purpose of these step is to subdivide a river in reaches, which are fundamental to properly analyze the geomorphology of a river. A reach represents the fundamental spatial unit, is the baseline for a proper characterization and functional for any of the following analysis. The process of subdivision is iterative and is performed by the individuation of macro-units until getting to the final subdivision of reaches. The step to identify reaches, described by Rinaldi et al. (2016) are the following:

1. Step One: physiographic units, which are macro-areas with relatively homogeneous physical characteristics, are defined. The principal factors taken into consideration are topographical elevations, geology, and vegetation cover. For each physiographic units segments can be defined. A segment corresponds to a macro-reach and is functional to the further identification of reaches. This units are defined based on the configuration of valley floor in terms of confinement, gradient gaps, and significant variations in flow discharge.
2. Step Two: the degree of lateral confinement, of the river's physiographic units and segments, is defined. The degree of channel confinement corresponds to the percentage of length of the river that has banks not directly in contact with the alluvial plain, but that touches slopes, landslide deposits, alluvial fans, old

fluvial terraces or glacial deposits. In other terms the degree of channel confinement describes the percentage of length in which there is the condition of confinement, with the impediment for the lateral mobility of the river.

3. The third step is to define the riverbed morphology. The morphological classification is based on different factors, such as the degree of channel confinement, the number of channels and the planimetric shape of the bed. Is important to point out that this step aims to define the morphology existing at the time of the analysis of the riverbed, even if it derives from artificial interventions. In this step is fundamental the definition of necessary indexes to the definition of fluvial morphology and of the width of the channel bed. The indexes analyzed are: braiding, anabranching and sinuosity indexes and will be deeply described in the following section.

   The bankfull channel is constituted by the portion of riverbed subject to morphological modifications, determined by bed material mobilization and transport. It is identifiable with active channels and bars.

4. The fourth point, and the last one, constitutes the final step for the subdivision of a river in homogeneous reaches, from a morphological point of view. With the previous step the main part should be already defined, and this last step is the final revision of the subdivision. For the subdivision these aspects are taken into consideration: discontinuity of the bottom slope, hydrological discontinuities: the presence of tributaries, morphological variations (such as frequency of bars or islands), variations of the alluvial plain dimensions, variations in sediments granulometry, strong artificialization (dams).

This process has not been applied in its integrity, a broad classification of river patterns has been performed, not considering morphological quality.

For sake of simplicity, what has been done, was the subdivision of reaches by analysing just the three specific indexes (described in the following chapter 3.1.3).

The aim was to have a first rough characterization of the morphology, and the identification of homogeneous reaches.

This was the baseline for satellite image classification, that has been performed on those reaches considered to be the most representative for their morphology. Each reach analysed has been selected by looking at the characterizing indexes values.

3.1.3 Indexes

In order to identify the morphology of river reaches, the identification of specific indexes is necessary. In this section they will be presented, and new indexes will be explained.

3.1.3.1 Sinuosity index (Si)

Is defined as the ratio between the length measured following the river flow (la) and the length measured following the direction of the overall watercourse planimetrical length (l1 + l2 + l3 + ...). it is utilized mainly to classify single channel riverbed, while is less significative for multiple channel rivers (Fig. 9).

It is mainly measured from satellite images, working on a GIS environment. The first step is to delimitate the riverbed. After having done it the centerline has to be characterized and is defined as the line equidistant from the riverbanks. The following step is to draw a line that represents the direction along which develops the planimetrical path of the river. These axis are taking into account all the significant variations of the direction of the river flow. When there is a change of the direction of the river a point of intersection with the river axe is identified (Fig. 9). The final step is to measure the length of the river between the two end of the reach and divide it by the correspondent length along the axis measured along the planimetrical path.

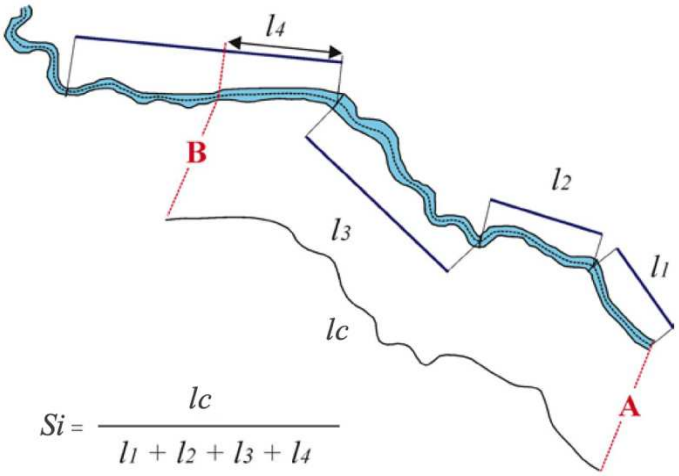

Fig. 9. *Measure of the sinuosity index of a river, between point A and B, with variations of the axis on the planimetrical path;. lc: length of the centerline, l1+...+l4: length measured on the planimetrical path.*

3.1.3.2 Braiding index (Bi)

Is defined as the number of active channels separated by bars (Rinaldi M. et al., 2015). It is used mainly to define riverbeds with braided and wandering channels, while is less important for the definition of single channel rivers or reaches. It is measured using satellite images on GIS environment. The procedures to calculate it are the following:

The first step is done on the riverbed axe where a spatial step is defined, in order to subdivide the axe in equal sections.

For each section the number of active channels is measured. The channels considered are those with a continuity in the flow discharge. This step can be affected by a certain degree of subjectivity, and by the levels of hydrometry that were present at the time in which the image was taken.

The final value of the braiding index corresponds with the medium value of the measures taken on the reach (Fig. 10.).

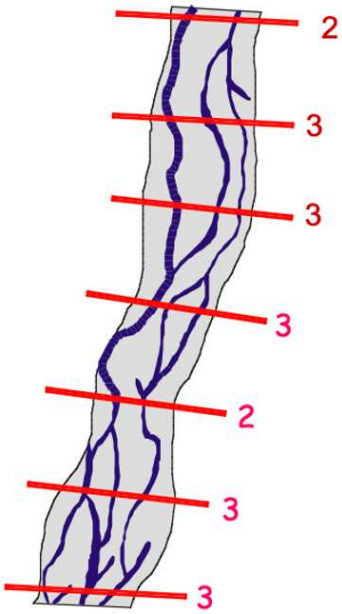

$$Bi = \frac{2+3+3+3+2+3+3}{7} = 2.7$$

Fig. 10. *Measure of the braiding index.*

3.1.3.3 Anabranching index (Ai)

Is defined as the number of active channels divided by island. It is used mainly to define anabranching riverbed, while is less significative for other single channel morphologies.

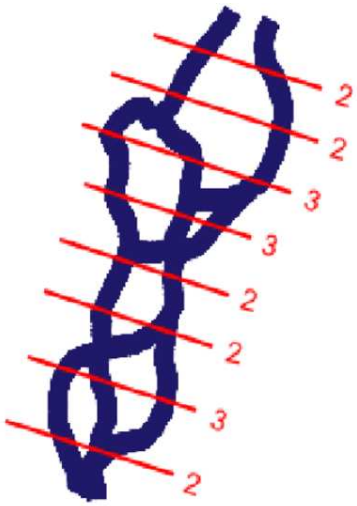

$$Ai = \frac{2+3+2+2+3+3+2+2}{8} = 2.38$$

Fig. 11. *Measure of the anabranching index.*

The measure of this index is done for wide riverbed (width > 30 m) and is similar to those for the calculation of the braiding index.

The difference is that instead of counting the number of active channels, are considered the active channels separated by islands. The final value of the anabranching index corresponds to the medium value of the measures done on the entire reach (Fig. 11).

In accordance with the three indexes described, which has to be implemented with other qualitative observations, will provide the definition of the final morphological pattern.

3.1.4 Morphological patterns

- *Straight:* Straight rivers are characterized by having a single channel, so with braiding index generally equal or close to 1, and with sinuosity index less than 1.05 (Brice J.C., 1975; Jean-René Malavoi & Jean-Paul Bravard, 2010). Generally are quite uncommon in natural environments, so are usually associate with artificial interventions.

- *Sinuous:* Sinuous rivers are characterized by a value of the sinuosity index higher than 1.05. there are further subdivisions inside this class but are irrelevant for the purpose of the thesis. Nevertheless important to mention that the threshold that gives the possibility to distinguish among sinuous and meandering rivers, for the sinuosity index, is 1.5 (Leopold L.B. & Wolman M.G., 1957).

  Both in sinuous and straight riverbeds there is the chance to have mainly lateral bars, that usually alternates on the two sides of the river. However, differently from transitional rivers, these bars are rarely present continuously through all the riverbanks and are generally less than 80-90% of the reach. Is possible to find islands, but the anabranching index is always generally low.

- *Meandering:* is a single channel (with braiding index usually equal or close to 1), characterized by sinuous trend, with the formation of one or more regular meanders. The principal parameter of characterization for this morphology is the sinuosity index, which has to be higher than 1.5 (Leopold L.B. & Wolman M.G., 1957). Is possible to go in deeper detail for this morphological

pattern but, as for sinuous reaches, is not necessary for the aim of this dissertation. Also in this case the anabranching index is generally low, even if some islands may be present.

- *Transitional:* morphologies that presents intermediate traits among the other categories fall in this class. For this reason is harder to univocally define threshold values with the three indexes, and also other characteristics are evaluated, some of them deriving from qualitative observations. The common characteristic is that transitional patterns is that they usually have a relatively wide and not very deep riverbed, mainly constituted by bars. The lateral bars' length in this type of river patterns is very high, usually higher than 90%. It means that the lateral bars are covering the whole length of the river. Within this class a further distinction among two members is required:
  1. Wandering: have a relatively wider riverbed, with diffused braiding parts, as well as islands and local anabranching patterns (the anabranching index can be higher than 1, but always lower than 1.5). This morphology describes situations that lay between meandering and braided channels.
  2. Sinuous with alternate bars: have characteristics similar to the previous, but the riverbed is generally narrower, and has fewer braiding patterns. They are characterized by an important difference between the low water channel and the main channel, with a narrow, sinuous channel that flows in a bankfull riverbed with low sinuosity (index between 1.05 and 1.45).

- *Anabranching:* are multi-channel riverbeds characterized by the presence of vegetated, or in general stable, islands that divides the flux into different branches. The multichannel is a constant feature, also during flood events. The anabranching index higher than 1.5 is characterizing for this pattern, the

braiding index is variable but normally close to 1, while the sinuosity index can be calculated for each channel and can be high but is not relevant.

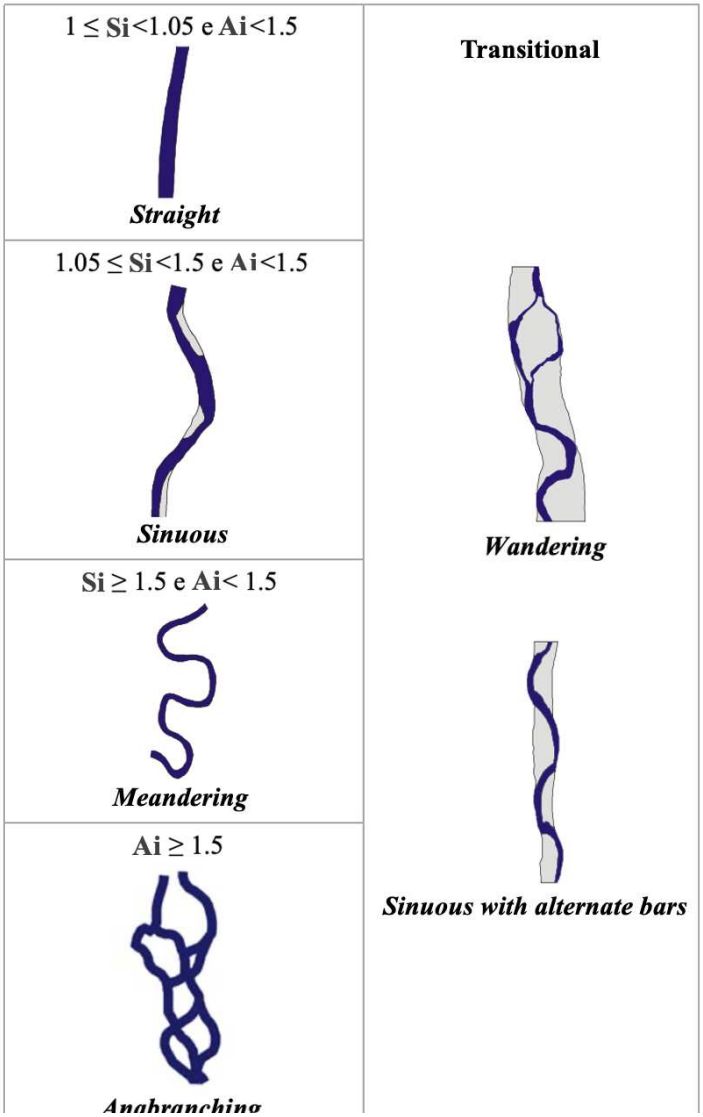

Fig. 12. *Scheme of the morphological patterns and their corresponding indexes.*

In the following table (Tab 1.) are presented threshold values for the utilized indexes for the definition of river morphologies. The distinction among different river patterns is rigorous for the distinction of sinuous, anabranching and meandering reaches, while for the transitional morphology is less strict. In fact is not possible to exactly discriminate threshold values but other type of more qualitative observations are required, such as the length of lateral bars, that normally has to be at least >80% of the reach.

Moreover is important to mention that not all the indexes are fundamental for the description of the typology of patterns, some are more important for a morphology than other, and vice versa.

MORPHOLOGY	SINUOSITY INDEX	BRAIDING INDEX	ANABRANCHING INDEX	OTHER DISTINCTIVE CHARACTERISTICS
Straight	**1** ≤ Si < **1.05**	1 – 1.5 (normally equal or close to 1)	1 – 1.5 (normally equal or close to 1)	The planimetrical path needs to be straight. Discontinuous presence (or absence) of lateral bars (length of lateral bars < 80%).
Sinuous	**1.05** ≤ Si < **1.5**	1 – 1.5 (normally equal or close to 1)	1 – 1.5 (normally equal or close to 1)	Discontinuous presence (or absence) of lateral bars (length of lateral bars < 80%).
Meandering	≥ **1.5**	1 – 1.5 (normally equal or close to 1)	1 – 1.5 (normally equal or close to 1)	
Transitional: Sinuous with alternate bars	<1.5	**1** < Bi ≤ **1.15***	Close to 1	Almost continuous presence of lateral bars (length of lateral bars > 80%). Compared to wandering patterns relatively narrower riverbed. No braiding and anabranching.
Transitional: Wandering	< 1.5	**1.15** < Bi < **1.5***	1 ≤ Ai < 1.5	Almost continuous presence of lateral bars (length of lateral bars > 80%). Compared to sinuous with alternate bars the riverbed is wider; significant braided or anabranching phenomena.
Anabranching	Any (also >1.5)	Any (also > 1.5)	≥ **1.5**	

Tab. 1. ***** *the threshold is discretional. Principal thresholds for the definition of river morphologies.*

3.1.5 Data collection

3.1.5.1 Indexes and morphological characteristics of the river

The area in which the morphological characterization has been performed goes from Torino to the Po delta. The data used for this classification has been based on the study conducted by Brenna et al., in 2022 in which the subdivions in reaches was performed in order to estimate changes in sediment flux.

The data has been provided to me by the research group headed by Bizzi S., that comprise Brenna A. and Bozzolan E.

From those data further analysis has been developed in a QGis environment. QGis is a GIS (Geographic Information System) software, free and open source, that allows to edit spatial data and to generate cartography.

Firstly an orthophoto of the whole length of Po River, has been acquired by the AdbPo in 2021, and uploaded and georeferenced on QGis. Moreover the high-resolution satellite image of 2020, present in the Software as basemap, has been implemented. Subsequently, thanks to the tools QGis provides, has been possible to get further information.

A raster for the whole Po to analyze has been created, as the centerline for the whole length. Thanks to the calculation functions many useful measures has been taken. In addition observation on the images has been done, in order to properly calculate the three characterizing indexes.

In Tab. 2 are defined: length of the centerline and length of the axis, both in meters, therefore the sinuosity index has been calculated, while for braiding and anabranching indexes the calculation has been performed by looking at the satellite images, following the methodology explained in the subchapters 3.1.3.2 and 3.1.3.3 (in Tab. 2. are reported just the values found).

From the values of the indexes has been possible to determine the morphology of each reach, and to evaluate the changes in the morphology itself. Has therefore been possible to properly define and identify each reach.

To perform a proper characterization of Po River, each reach has been compared both with Tab. 1 and with graphs, to describe the properties of each morphology.

The following parameters that has been calculated are the riverbed area (m^2) and the area of the islands (m^2), which are fundamental to define width of the active channel (m). The width of the active channel (Acw) is calculated by subtracting the area of the islands (Ia) from the riverbed area (Ra), subdividing it by the centerline length (lc):

$$Acw = \frac{Ia\ (m^2)\ -\ Ra\ (m^2)}{lc\ (m)}$$

This value is useful for further analysis.

The information obtained following the next steps are fundamental to find a functional link between the calculated indexes and the morphology drivers.

3.1.5.2 Normalized drainage area (W)*

Analysis carried out by Piégay et al., (2009) showed that the active channel width can be related to the catchment size in order to provide a normalized value. The W* is a proxy related to the sediment supply (if we compare two rivers that have the same drainage area above, the highest value corresponds to a bigger sediment supply).

This variable has been calculated in a GIS environment, following these steps:

- Download of a DEM (Digital Elevation Model), with a spatial resolution of 500m of the Po River basin, with EPSG:32632 - WGS 84 / UTM zone 32N as coordinate reference system.

  The DEM has to be preprocessed in order to produce hydrological flow models. This passage produces an elevation dataset which is free from "sinks" or depressions that could capture the flow of water. To produce a filled DEM is used a SAGA function on QGis, called fill sinks (Wang and Liu) that is found by looking at *Terrain Analysis>Preprocessing>Fill Sinks (Wang Liu)*. The DEM of the Po River has been used as input, and a filled elevation dataset has been created.

- The next step is to use the Flow Accumulation tool that calculates the accumulated flow. the first step done by the tool is to create the flow direction, which shows the direction of travel from each cell. Afterward a number is assigned to each cell that represents the number of cells that flow into each cell. The value of cells in the output raster is given by the sum of the cells that flow into each cell. Cells with a high flow accumulation are areas of concentrated flow and cells with a flow accumulation of 0 are topographic highs.

  The tool can be found in the SAGA package and is called Flow Accumulation (Top – Down). The filled DEM is used as input, to provide a flow accumulation cleared from sinks.

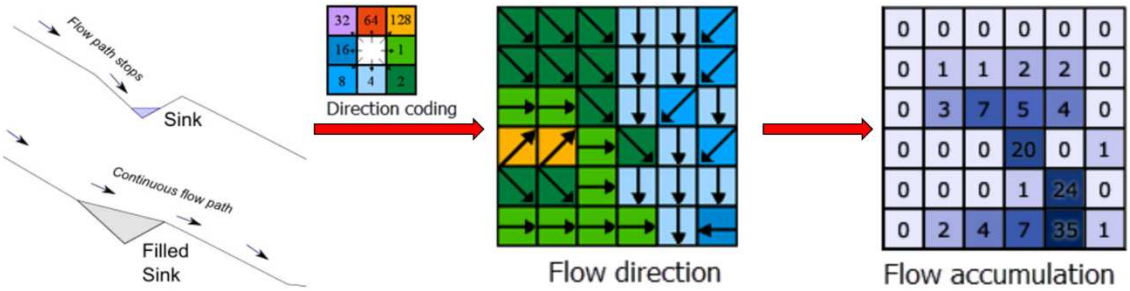

Fig. 13. Visual representation of the Fill sink (Wang Liu), flow direction and accumulation algorithms (ArcGIS Pro 3.1, n.d.; SAGA, n.d.).

- The next step is to manually analyze the flow accumulation produced and identify for each reach the pixel that has the highest value (hpv).

- In order to find the drained area (da) is necessary to multiply this value for the area of a single pixel. Since the spatial resolution of the DEM used was of 500m, the area of a pixel is 250000. To have numbers that are easier to deal with, the measurement units has been changed from m^2 to km^2, by multiplying the result for 10^{-6}.

- Finally the normalized drainage area (W*) has been calculated by dividing the width of the active channel for the drained area.

3.1.5.3 Slope (S)

The slope calculation has been the last performed, still in a QGis environment.

The calculation is simple, the first step is to identify, on the DEM, the height of the upstream and downstream end points of the reach, than the elevation difference between the two points has to be divided by the length of the reach (Cohen et al., 2018). Slope is usually expressed in percentage, to better deal with the data.

From data of slope and normalized drainage area is possible to build significative a graph that confront the two datasets.

REACH	lc (m)	l axe (m)	SINUOSITY INDEX	BRAIDING INDEX	ANABRANCHING INDEX	MORPHOLOGY	MOTIVATION FOR THE CHANGE OF THE REACH	RIVERBED AREA (m^2)	AREA OF THE ISLANDS (m^2)	ACTIVE CHANNEL WIDTH (m)	DRAINED AREA	NORMALIZED DRAINAGE AREA (W*)	SLOPE
PO_1	3678	3347	1,10	1,00	1,57	Anabranching	S. Mauro Torinese dam	1208054	529598	184,4710829	8604	0,021440154	0,1087593
PO_2	5980	5237	1,14	1,08	1,00	Sinuous	Riverbed widening; Allargamento alveo; increasing in channels and islands	791677	56330	122,9595891	8719,75	0,014101275	0,2340982
PO_3	7933	7186	1,10	1,06	1,24	Sinuous with alternate bars	Orco Stream confluence	2031884	352709	211,6749209	10192	0,020768732	0,1512707
PO_4	8619	8057	1,07	1,16	1,00	Wandering	Riverbed widening; Allargamento alveo; increasing in channels and islands	1710110	76549	189,5337055	10358	0,018298292	0,1624348
PO_5	5794	5426	1,07	1,21	1,57	Anabranching	Dora Baltea confluence	2512057	877329	282,1351504	10424	0,02706592	0,1553296
PO_6	6412	6030	1,06	1,43	1,21	Wandering	Narrowing of the riverbed; decrease in extent and number of bars	2261629	527478	270,4610717	15033,75	0,01799026	0,1715578
PO_7	5944	5639	1,05	1,07	1,00	Sinuous with alternate bars	Increase in sinuosity	1318914	104165	204,3672513	15277	0,013377447	0,0841191
PO_8	22108	17745	1,25	1,20	1,07	Wandering	Lanza dam; decrease in turns radius and sinuosity	4448839	121546	195,7332674	15619,75	0,01253114	0,1221271
PO_9	5386	4863	1,11	1,20	1,00	Wandering	Sinuosity increase and apperance of bars	942786	0	175,0399	15696,25	0,011151702	0,2227949
PO_10	8982	7233	1,24	1,07	1,22	Sinuous	Sesia River confluence; increase in channel number	1909525	230646	186,9212494	19586,5	0,009543372	0,0222674
PO_11	19683	16589	1,19	1,41	1,31	Wandering	Narrowing of the riverbed; decrease of channels number and increase in sinuosity	9412344	1581240	397,8711884	20020,25	0,019873438	0,0914517
PO_12	6830	5120	1,33	1,08	1,08	Sinuous	Tanaro River confluence	2000491	147212	271,3587214	29347	0,009246557	0,0732104
PO_13	7820	7370	1,06	1,25	1,19	Wandering	Geometry of the bars' modification; increase in number of channels	3391774	324611	392,2029177	29645	0,013229985	0,0511486
PO_14	18228	16952	1,08	1,46	1,16	Wandering	Narrowing of the riverbed; decrease extent and number of bars	10606675	790554	538,5269746	32254,75	0,016696052	0,0822922
PO_15	17048	14933	1,14	1,24	1,03	Wandering	Ticino River confluence	5444633	5148	319,0656349	38568	0,008272807	0,0175972
PO_16	11857	10817	1,10	1,15	1,25	Wandering	Decrease in sinuosity	5965132	140099	491,2705812	38748,5	0,012678441	0,0337351
PO_17	9955	9717	1,02	1,07	1,07	Straight	Increase in sinuosity	4272049	198273	409,2087245	39794,5	0,010283047	0,0100449
PO_18	34800	16742	2,08	1,04	1,07	Meandering	Trebbia River confluence	12230552	323377	342,1575617	43729,5	0,007824411	0,0201148
PO_19	30954	17250	1,79	1,03	1,15	Meandering	Serafini Isle dam	10713473	905550	316,8501801	44813,75	0,007070379	0,0258444
PO_20	9076	8122	1,12	1,11	1,89	Anabranching	decrease in number of channels; desapperance of islands	22453832	15519033	764,0426511	53690,25	0,014230566	0,0330526
PO_21	12177	11495	1,06	1,07	1,00	Sinuous	Arda Stream confluence	3737070	0	306,908342	54210,5	0,005661419	0,0164251
PO_22	10201	8786	1,16	1,00	1,08	Sinuous	Decrease in sinuosity	3161537	43264	305,6908514	54402,25	0,005619085	0,0000000
PO_23	9058	8168	1,11	1,00	1,25	Sinuous	Taro River confluence	5063711	1734589	367,5403675	56772,75	0,006473887	0,0000000
PO_24	7604	7156	1,06	1,00	1,10	Sinuous	Increase in sinuosity	3735939	889670	374,2924344	56842,5	0,006584729	0,0657514
PO_25	13202	9222	1,43	1,00	1,18	Sinuous	Parma Stream confluence; decrease in the radius of bends	6752970	2545525	318,6984646	57902,5	0,005504054	0,0151493
PO_26	17506	15203	1,15	1,04	1,08	Sinuous	Increase in the extent of bars	6983636	2137782	276,8039838	58965	0,004694378	0,0114244
PO_27	15269	12700	1,20	1,00	1,26	Sinuous	Oglio River confluence; iincrease in bars number	7125599	1350718	378,2051975	59784,75	0,006326115	0,0065491
PO_28	15111	14033	1,08	1,36	1,36	Wandering	Increase in the radius of bends	8740548	1774656	460,9943423	67606,75	0,006818762	0,0397073
PO_29	13866	10479	1,32	1,11	1,11	Sinuous	Mincio River confluence	6241180	922199	383,5948854	71239,5	0,005384581	0,0144236
PO_30	11622	10652	1,09	1,00	1,25	Sinuous	Increase in sinuosity	5219305	400930	414,5987268	73992	0,005603291	0,0086045
PO_31	20646	13495	1,53	1,04	1,15	Meandering	Decrease in sinuosity	9246603	1026998	398,1180804	74165,75	0,005367951	0,0145306
PO_32	17542	15433	1,14	1,14	1,10	Sinuous	Panaro river confluence	8729101	418675	473,7363823	76776,25	0,006170351	0,0057005
PO_33	17852	15490	1,15	1,10	1,10	Sinuous	Pontelagoscuro: traditional threhold	8222726	486865	433,3214807	76944,25	0,005631629	0,0056015
PO_34	18017	15949	1,13	1,00	1,06	Sinuous	Disapperance of emerged bars	7284142	35547	402,3093802	77123,5	0,005216431	0,0055502
PO_35	22271	20824	1,07	1,00	1,05	Sinuous	Po di Goro inlet	8001294	31922	357,8410809	77356,75	0,004625855	0,0044902

Tab. 2. *Data acquired on the Po river. Each reach is defined as "PO_" and a number.*

3.2 Satellite images classification

3.2.1 Image selection: Sentinel 2

Sentinel-2 is the name of an ESA (European Space Agency) mission started in 2015, with the aim of monitoring changes in land surfaces. In order to achieve the result, two satellites characterized by a wide swath (290 km), high resolution, multi-spectral imaging and a high revisiting frequency of 5 days for Europe.

The two polar orbiting satellites are placed in the same sun-synchronous orbit, phased at 180° to each other. This satellites acquire multispectral images, thanks to a specific instrument (MultiSpectral Instrument -MSI), which acquires 13 spectral bands. MSI collects sunlight reflected or absorbed and re-emitted as thermal infrared wavelengths, by the Earth's surface. This kind of acquisitions defined as "passive" because it measures the energy that is naturally available and, is different from the active acquisition that detects the variations given by interference of the radiations provided by the sensor with the surface (ESA, 2015).

All Sentinel-2 data are freely available weekly at a maximum resolution of 10 meters.

As said by (Bozzolan Elisa et al., 2023 - under revision) machine learning algorithms on satellite images, in this case Sentinel 2, are opening the opportunity to automatically classify and monitor fluvial geomorphic features and processes.

Sentinel 2 images have been downloaded from the European Space Agency (ESA) Open-Access Copernicus hub, starting from January 2018, until December 2022. The aim was to extract information on the adjustments between water, sediment and vegetation, in the active channel of Po River, throughout a period of 5 years.

The three classes are pretty well discernable from each other because have different spectral behaviors.

3.2.2 Fuzzy classification:

Fuzzy classifications try to infer sub-pixel composition by giving an "affiliation" percentage to each pixel for each class. The method is based on the spectral behavior

of each component of a class, that behaves differently when hit by sunlight (see subchapter 3.2.2).

By unmixing a pixel into its component parts it is possible to enable more accurate estimation of the areal extent of different land cover classes (Carbonneau et al., 2020).

Another important aspect is that, in this case, fuzzy classifications can mitigate the low spatial resolution of Sentinel 2 images.

The fuzzy classification performed by Carbonneau et al., (2020) has been based on low-cost drones, unmanned aerial vehicles (UAVs), that acted as ground truth to generate high quality training data for the fuzzy classification algorithms, applicable to Sentinel-2 imagery. This classification considers three end-member classes: water, vegetation and dry exposed sediment (named just “sediment” for the sake of simplicity).

For all of the reaches, that have been selected to be analyzed (because considered to be the most representative for their morphological class) a fuzzy classification from January 2018 to December 2022 has been performed.

The output of it, are NetCDF (network Common Data Form) files. NetCDF is a file format that stores multidimensional data, in this case the values for each class through each month (UCAR, 2023). An example of the output is presented in Fig. 14. a, b and c, that represent respectively pixels classified as water, sediment and vegetation for reach 5 in January 2018.

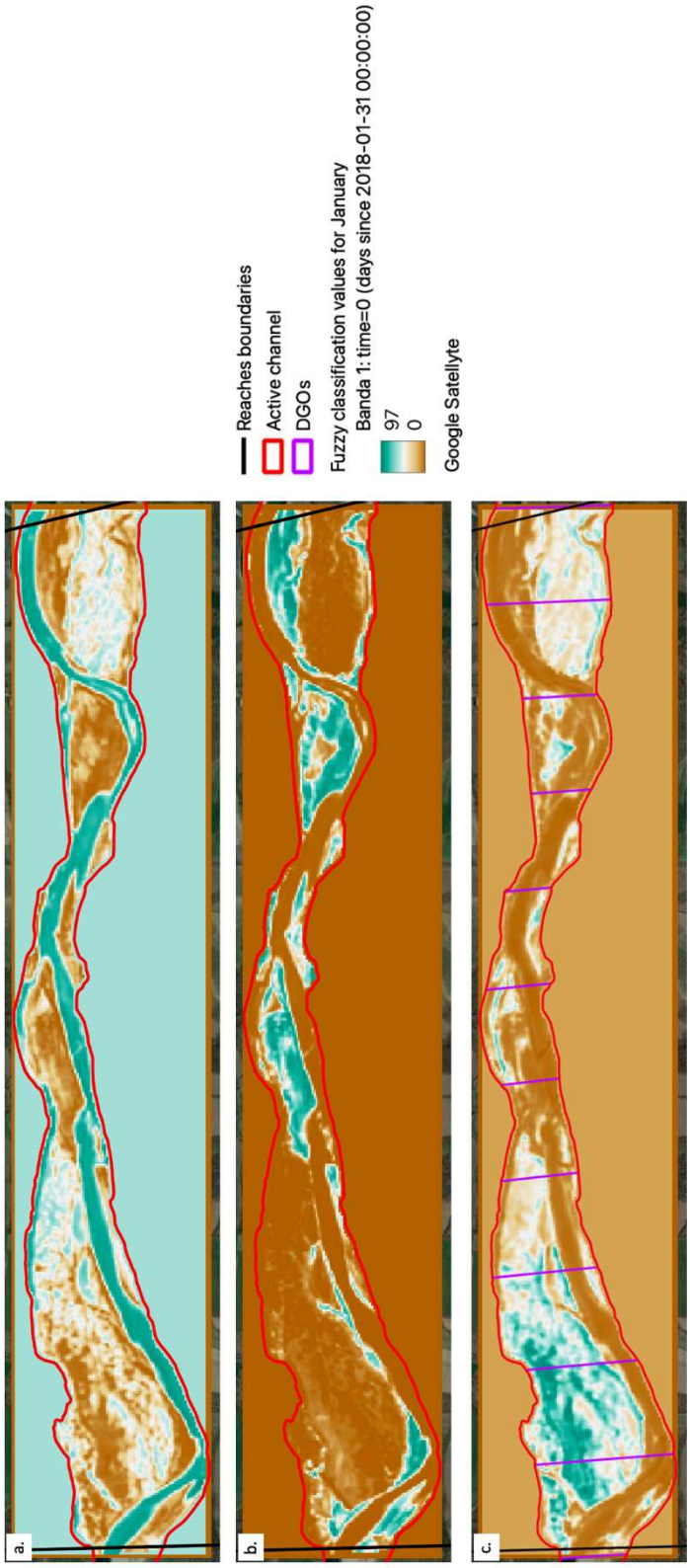

Fig. 14. *Fuzzy classification for reach 5, in January; a. pixel values for water class; b. pixel values for sediment class; pixel values for vegetation class. In red the active channel is evidenced, and the black lines determines the reach boundaries.*

3.2.4 Python code for satellite-images classification

The production of a satellite image classification has been performed in a Spyder environment, through the Anaconda Data Science platform. Spyder is a free, open-source scientific environment written in Python (programming language).

The code has been developed by Micotti M. and modified by Bozzolan E. in 2023 and is composed of three main parts.

The first part corresponds with the loading of the fuzzy classifications for the three classes, for all the years to analyse. Then a shapefile with DGOs has to be upload (Fig. 14 c.).

DGO stays for Disaggregated Geographical Object and aims to characterize a reach with high spatial resolution continuously (Alber & Piégay, 2011).

DGOs have been created by the implementation of Fluvial Corridor Toolbox Package in QGis, and corresponds to areas 500 meters wide (Roux et al., 2015).

The third part constitutes the main section of the code, where the effective analysis of date is performed. In this part functions present in the second section are recalled.

The output provided is constituted by a barplot and a lineplot that represents the trends of all the three classes for the years they have been analysed with fuzzy classification, each of them has been clipped on the DGOs.

This code has the capability to provide outputs for each DGO, giving the chance to create a much more punctual analysis of the river. What has been produced here is an output that comprehend the analysis of each DGO, aggregated to create a unique output for the reach we wanted to analyse.

The code has the potentiality to also produce outputs for each DGO, therefore verify information every 500 m for Po River.

4. Results and Discussion

4.1 Traditional classification

Through the kilometers that separates the starting from the ending point, the river has been analyzed, and subdivided into 35 reaches, based on indexes and on observations. In Fig. 15 are represented the classified reaches, and where they are located.

The graph on the right side represent the percentages of each morphology recognized. The majority of reaches has been classified as sinuous this class represents the 46% of the total. The second most frequent class is constituted by the transitional morphology, comprehensive of both wandering and sinuous with lateral bars reaches. As we observe from spatial distribution, in fact they are usually more common where grain size is gravel and/or gravel and sand. Whereas sinuous morphologies are found going downstream towards the Po delta, where sand grainsize is the dominant.

The other morphologies accounts for 20% of the total.

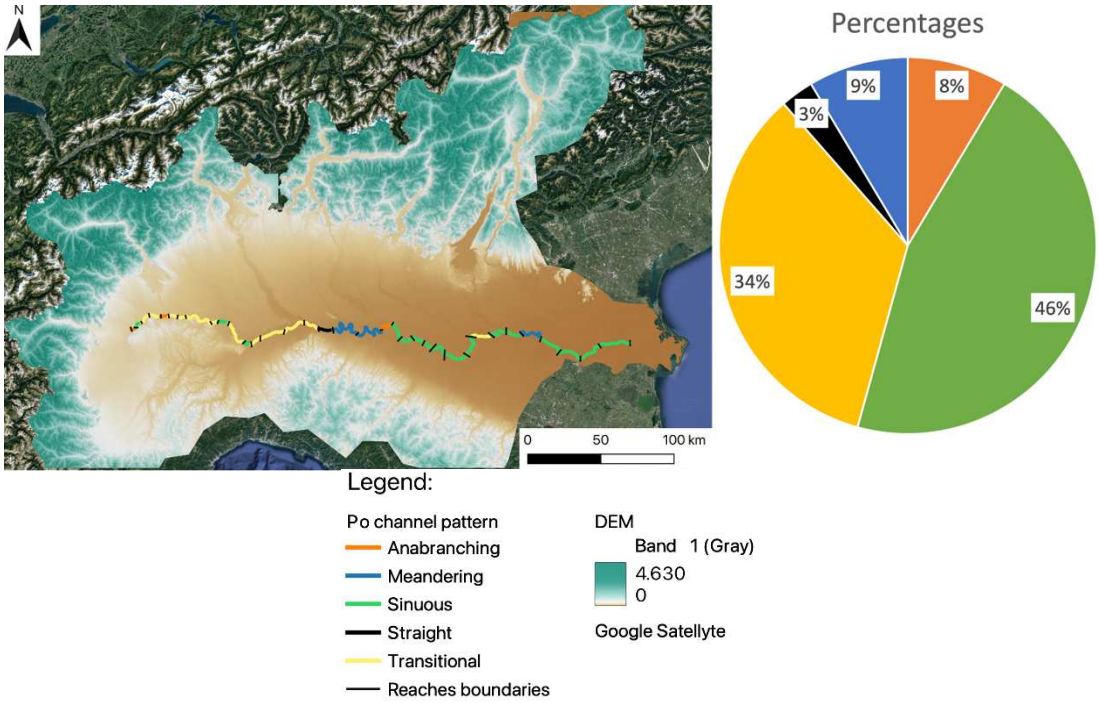

Fig. 15. *On the left, spatial distribution of reaches; on the right percentages of morphologies within the reaches.*

In Fig. 16 are presented the most iconic reaches for each morphology. They have been chosen to be the representatives of their geomorphological patterns thanks to observations done, comparing the various indexes found.

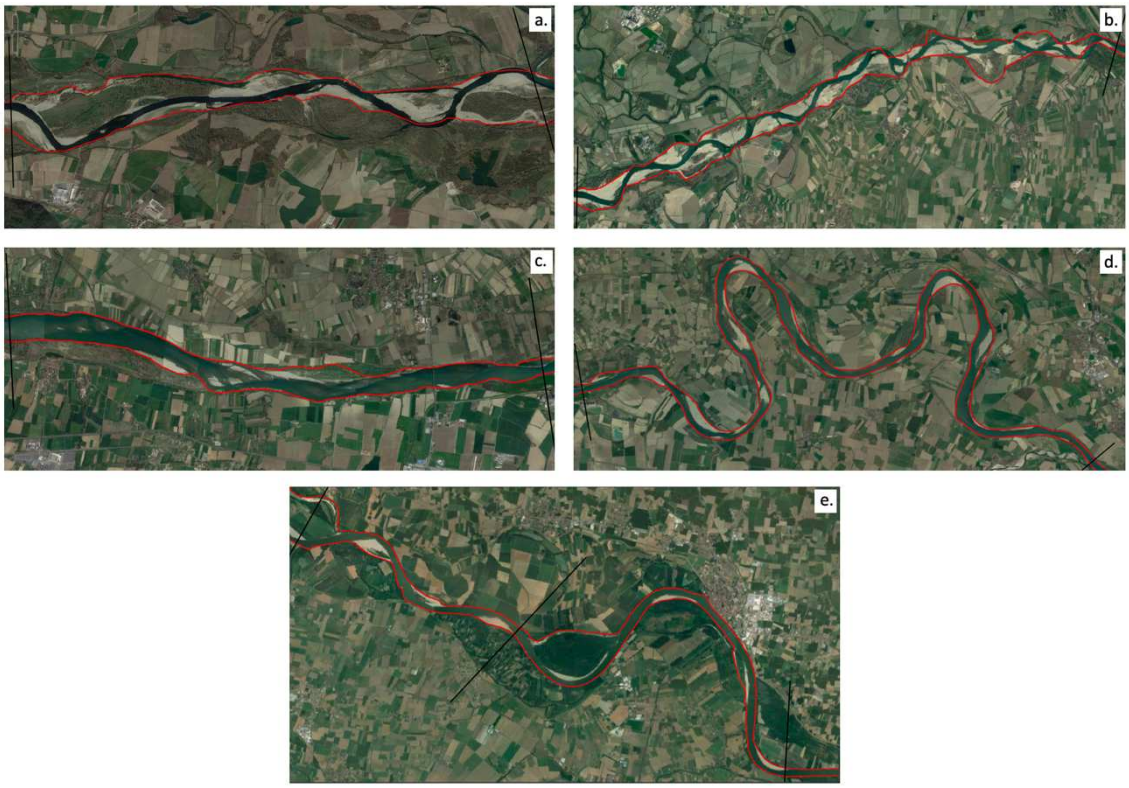

Fig. 16. *In the images are presented all the morphologies analyzed; a. reach number 5, anabranching; b. reach number 14, transitional; c. reach number 17 straight; d. reach number 18 meandering; e. reach 24 and 25, sinuous.*

Fig. 17. compare the sinuosity with anabranching and braiding indexes. The easiest morphology to recognize is without any doubt the meandering type. In fact it is characterized by low values in both anabranching and braiding indexes, and very high values for sinuosity index.

The second most recognizable morphology is the straight pattern. This morphology is not very common in a natural environment but can easily be found in a very confined and anthropized environment. This is what we can observe also in this case. If we have a look at Fig. 16 (b) we can see that the active channel is bounded by artificial margins,

built to guarantee mor space to croplands and small towns. In such a confined riverbed the only possible morphology to have, is to behave as straight. It has to point out, though, that just one reach has been inserted in this class, therefore it might be not so representative of the whole category. Nevertheless in this frame it is easily discernable from other morphologies because it has low values in each and every indexes.

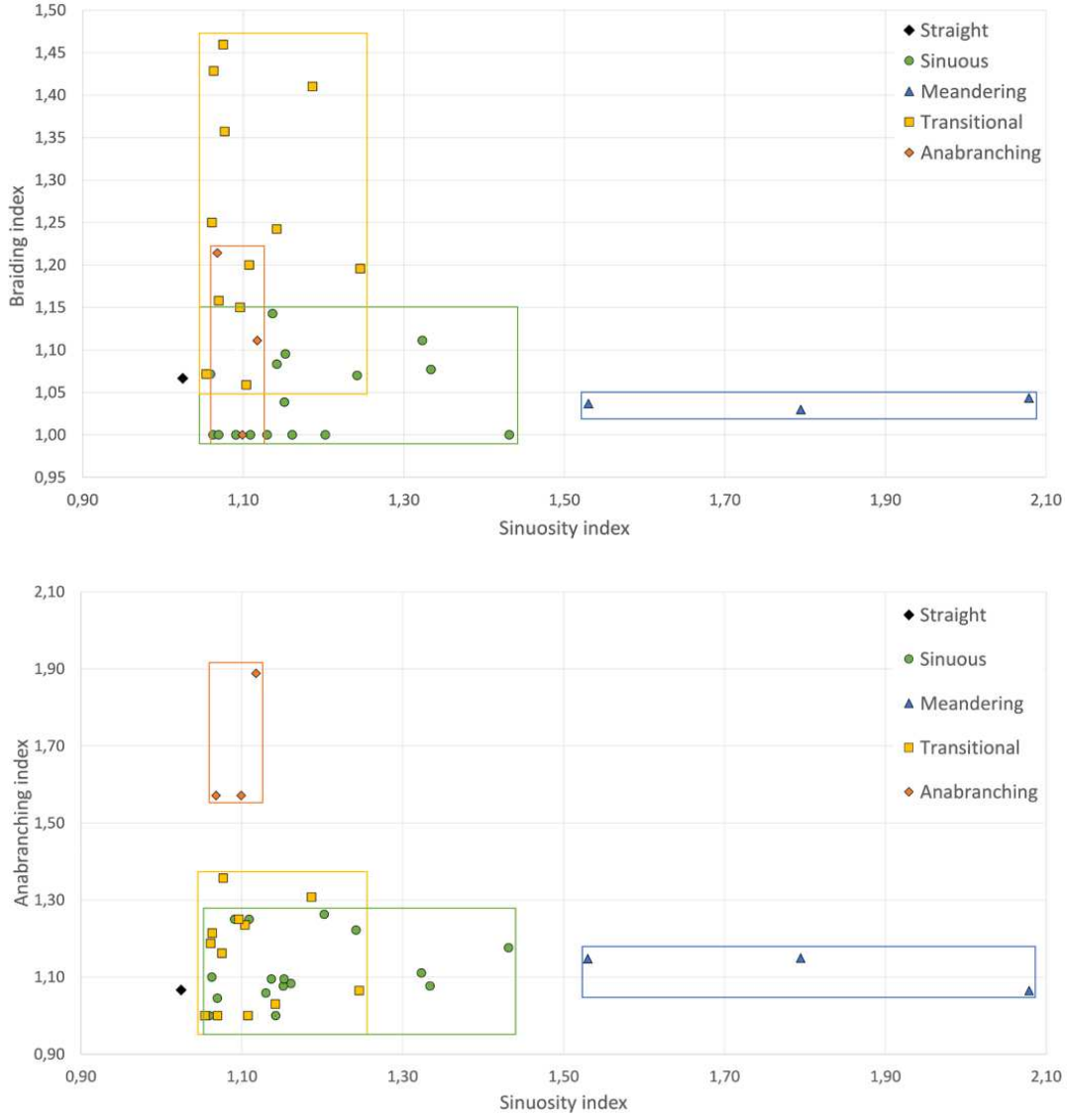

Fig. 17. *Comparison of the three morphological indexes, for the recognition of classes and eventual outliers.*

The third recognizable class is the anabranching, thanks to the high values in anabranching index.

The last two classes, transitional and sinuous, are difficult to separate, because both have quite a wide range of values in all the three indexes. It is clear though that for the sinuosity index both lays under 1.5 value.

Given these difficulties in the distinction among two classes, a further clarification has to be done. In fact if we look at the graphs and consider the classes as they are, is impossible to distinguish among sinuous and transitional reaches.

In the following graphs a more detailed distinction has been applied, taking into consideration the subdivions of transitional morphologies into wandering and sinuous with alternate bars.

As we can see from Fig. 18, now the distinction between the two morphologies is easier: the wandering patterns lies above the red dashed line, that corresponds to the value of 1.15 for the braiding index.

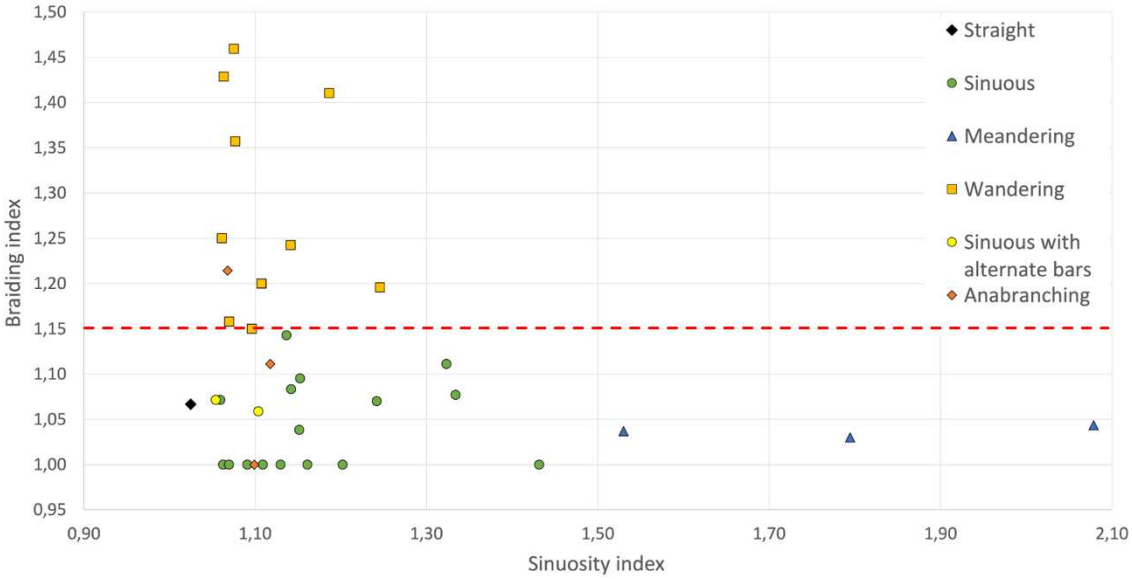

Fig. 18. *This graphs takes into consideration the further distinction of transitional patterns. The red dashed line corresponds with 1.15 value of braiding index and marks the threshold for the distinction among wandering and sinuous morphologies.*

The question now is: why do we have the two reaches that has been classified as transitional, in particular sinuous with alternate bars, that lies below the dashed line?

This morphology is included in the transitional patterns. Transitional morphologies usually are characterized by multi-channels, that forms because have to accommodate a lot of sediment. Sinuous with alternate bars patterns accommodate high amounts of sediments, but the conformation they assume is constituted by a single channel. Therefore the braiding index is comparable to strictly sensum sinuous reaches.

The difference between the two river morphologies can be identified by looking at the area, and in particular at river bars. For the sinuous with alternate bars pattern, in fact, when the up-flow bar finishes, the downflow bar starts, they are formed in continuity one to each other. On the other hand for sinuous patterns bars are not in spatial continuity. This is the principal reason because we can find sinuous with alternate bars that lays within sinuous reaches.

A further example of the thin distinction between the two classes can be found by having a look at Fig. 19.

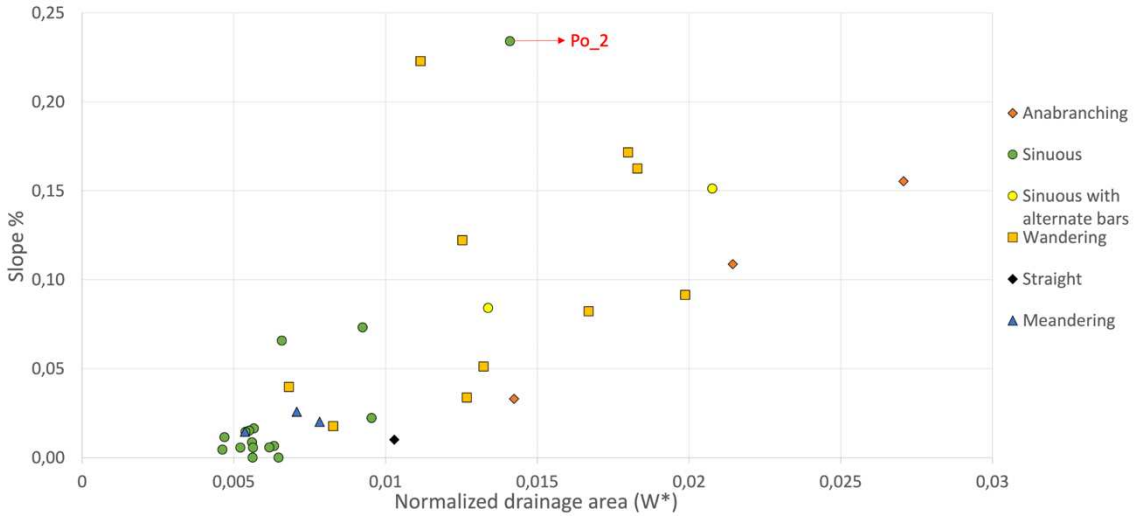

Fig. 19. *Graph representing the distribution of morphology of the reaches compared to the slope and the normalized drainage area.*

The chart has on the x axes the normalized drainage area W* (see subchapter 3.1.5.2), and on the y axes the slope (see subchapter 3.1.5.3).

W* is a proxy linked with sediment supply, and if compared with slope provide us important information. It is clear that anabranching and wandering morphologies, which

are characterized by multiple channel patterns, have higher values of W*, if compared to sinuous, straight and meandering morphologies, that, on the other hand, are characterized by a single-channel pattern.

This means they have a wider channel width for the same catchment area upstream, therefore they have to accommodate higher amounts of sediment supply for the same upstream drained area, as reported by many authors (e.g. Liébault et al., 2013).

Is interesting that W*, which has not been used to define morphology, actually can provide a tool to discern different patterns. The discriminant power of this proxy is that for each morphology it can give us a hint on the channel process, which define channel sections, morphological unit configurations and their dynamics overtime.

By having a look at fig. 19 there is just an outlier, for which what have been said before seems not to work. In fact Po_2, that is classified as sinuous, seems to behave as transitional. Why does this happen?

The first consideration to be done is that the DEM used has a spatial resolution of 500 m. This low resolution can affect the slope calculations, and therefore give a misleading output. But if we have a closer look to the reach, we can easily understand why there is this apparent discordance between the dataset and the effective situation.

In Fig. 17, on the left there is Po_2 reach, while on the right Po_3 reach has been reported. As we can see the two doesn't differ much. One thing is certain though, Po_2 doesn't have continuous bars, but they are interrupted for some meters, before the next bar starts again. Therefore the outlier actually has been well classified.

What is pointed out here is that the transition between different river morphologies can't be defined by sharp threshold. The reality is that in nature there are always gradual transitions from one pattern to another (Gurnell et al., 2009).

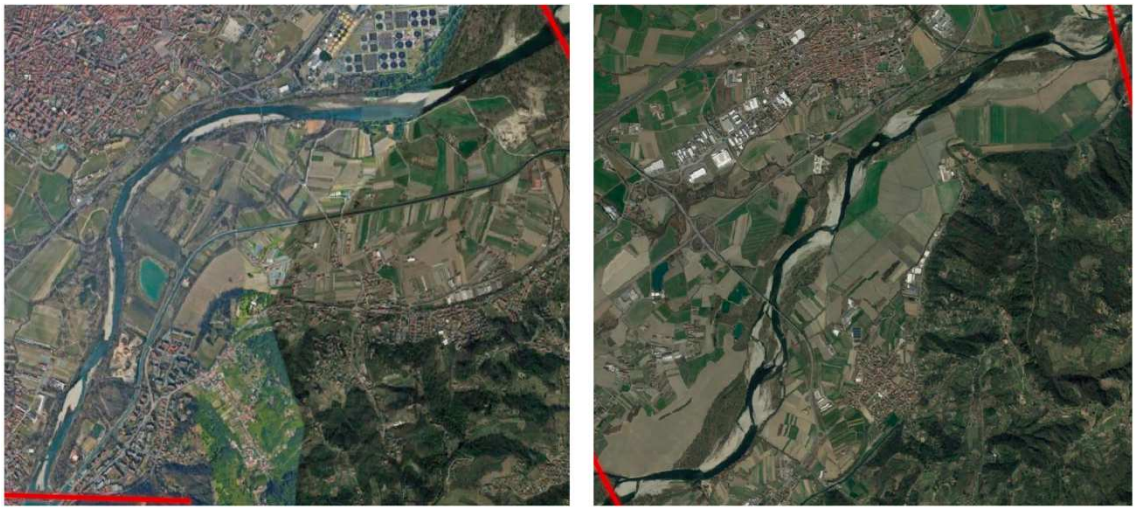

Fig. 20. *On the left Po_2, classified as sinuous reach; on the right Po_3 reach, classified as sinuous with alternate bars reach. The red line indicates the starting and ending point found for the identification of the reach.*

4.2 Satellite images classification

The second and most innovative part of this thesis is constituted by the implementation of a satellite-image based classification.

The traditional classification not only gave us a chance to analyze the Po River by the use of indexes, but it has allowed to determine the most representative reaches, for each morphological class. This is the baseline for the satellite image classification, that has been performed only on those identified reaches. Satellite imagery having higher frequency of acquisitions (up to five in a month, not considering clouds) allow to test macro-geomorphic units dynamics within river reaches previously defined, enhancing our ability to characterize river morphology and their associated geomorphic processes. In Fig. 16. the reaches have been presented. It is important to point out that a further observation has been done, to verify that all the reaches chosen were the most suitable for the analysis: all the reaches have to be the least anthropized possible so that their

geomorphic dynamic and distribution of geomorphic units is less affected by anthropic pressures and characteristic of the specific river morphology.

If we have a look at graph 15. b. we can notice that the most separate (therefore easily discernable from other classes) value for the anabranching morphology, is constituted by the reach 20 (see Tab. 2.).

If we examine that specific reach (Fig. 21.) we will see that it actually comprises Serafini Island, and an artificial channel. Isola Serafini is famous for its dam built in 1958 that diverts water from the main meander into the artificial cut-off. In this very anthropized area a comparison between satellite-image classification loses its significance. It is important to test the method in pristine river reach, so to be able to characterize morphological processes in absence of notable anthropic impacts. For this reason the anabranching reach chosen is the number 5 (Fig. 16 a.).

After this first evaluation, Sentinel-2 images have been downloaded (see subchapter 3.2.1), and the fuzzy classification has been performed (see subchapter 3.2.2).

The output of the fuzzy classification consists in a NetCDF file that shows the percentages of a class through different months. For each reach, from 2018 to 2022, NetCDF files has been produced for all the three semantic classes: water, sediment, vegetation. Each of them has been used to run the code created by Micotti M. and

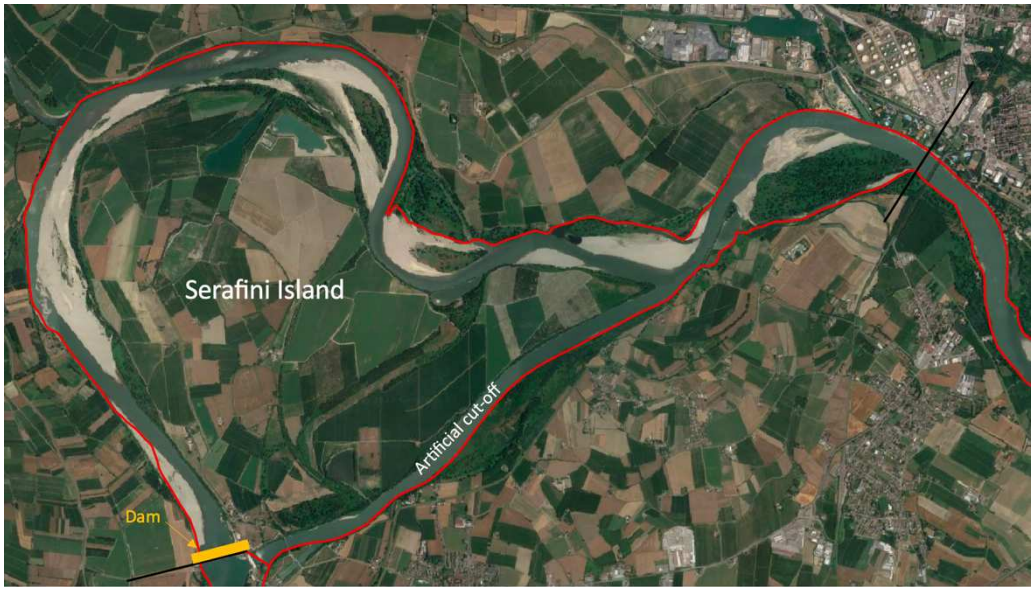

Fig. 21. *Reach 20, as we can see is a very complex area with the dam of Isola Serafini and the artificial cut-off. Is not the most suitable reach to analyze in this context of research.*

modified by Drs. Bozzolan E. and provided me by the research group in Padova in order to create graphs that shows the trend of the three semantic classes throughout all the years to analyze.

4.2.1 Temporal variations of the three semantic classes

Here below are presented all the graphs for each reach.

All the graphs presents on the x axis the time, and on the y axis the classified percentages of the three semantic classes: water, sediment and vegetation. As we can see not all of them contains all the months that we aimed to analyze. This unbalance is due to the available data we have been able to collect.

In fact the satellite images suitable for the analysis has been those with a cloud coverage maximum of 35% of the total image. This percentage has been tested during the process of creation of fuzzy images. In the beginning the percentage used was 20, but it has been seen that too many images were discarded.

Moreover difficulties in the download of Sentinel-2 images have been encountered. Therefore some months are missing, but overall the analysis is satisfactory, because has been able most of the months in a period of five years.

4.2.1.1 Anabranching morphologies: temporal variations

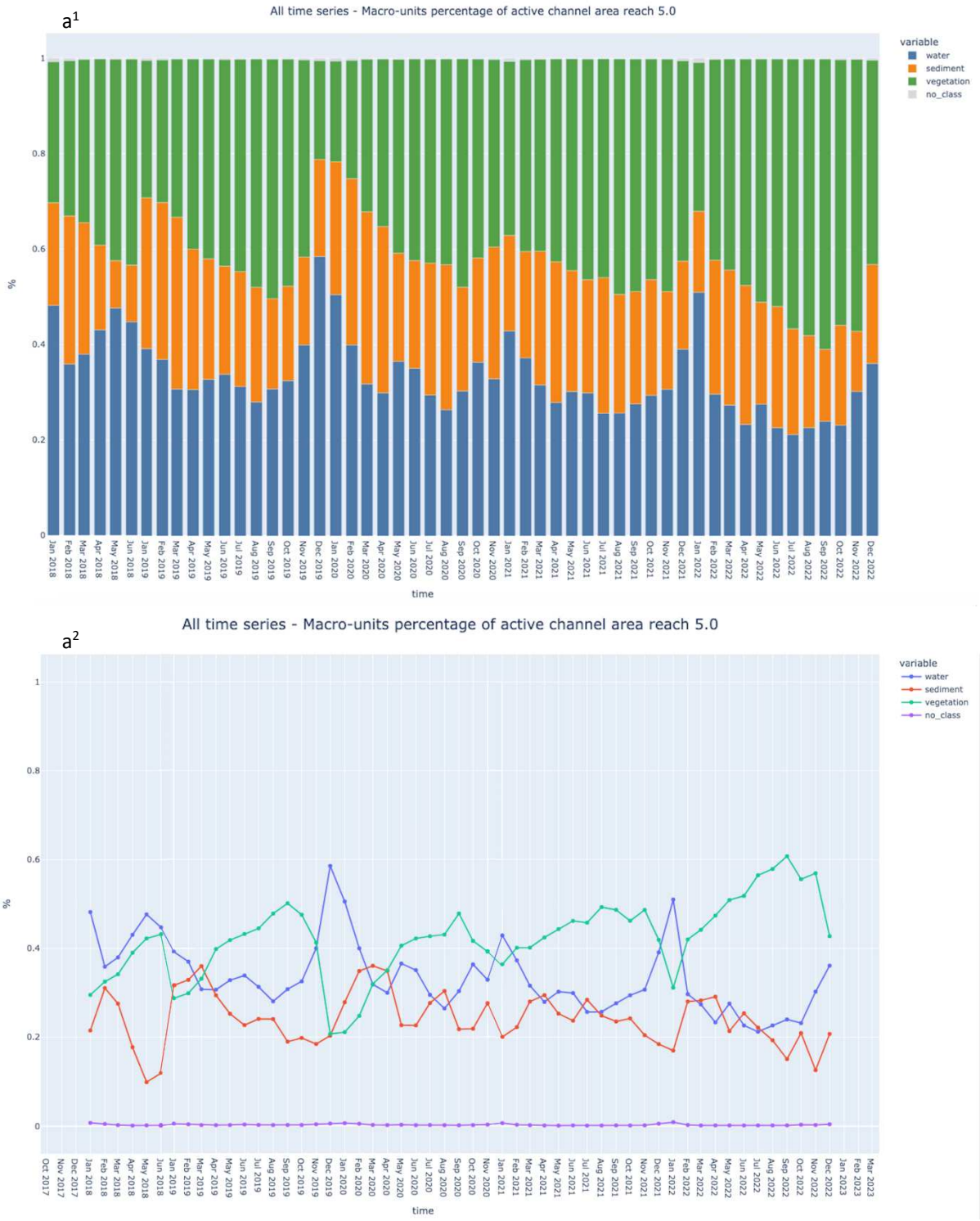

Fig. 22. Trends from January 2018 to December 2022 of water, sediment and vegetation for reach 5; a1 bar plot with water classified in blue, sediment in orange and vegetation in green; a2 lineplot with water in blue, sediment in red and vegetation in green, in *purple there is a line for the non-classified pixels.*

In Fig. 22 are presented on top bar plots and below line plots, with the variation of percentages of the three classes through time. Figure a^1 and a^2 is referred to the reach number 5 (Fig. 16, characterized by the traditional classification as anabranching.

Let's analyze class by class the information provided, starting from water.

In general there is a recognizable trend of diminution of water throughout the 5 years, with the lowest point of 22% of water, reached in July 2022. This path falls into the extreme drought the Po River experienced in that year, during which some of the minimum peaks for water of the last 50 years has been reached.

If we have a closer look some seasonal trends are recognizable too. In fact water conditions are characterized by quite intense peaks, in the order of 10% variation, reached during winter season (around December-January), and some minor peaks around May. The highest peak of these five years analyzed is reached in December 2019 with a value of 59% of pixels classified as water. Arpae (Regional Agency for Prevention, Environment and Energy of Emilia-Romagna Region) registered a significative flood event halfway between November and December (Riccardi Giuseppe & Comune Elisa, 2019). The seasonal minimum are achieved around March-April and July-August. For what concerns sediment class, there are recognizable trends as for water. This class is characterized by a certain degree of stability. The lowest value is encountered in 2018, followed by and increase until reaching 26% in 2020, and another decrease down to 2022 (Tab. 3.).

As a general observation these fluctuations can be linked mainly with high flow events, which the only noteworthy occurred in December 2019. In general maximum peaks are registered around March, and August. During these months usually precipitations are not so strong, and therefore sediment is exposed. On the other hand minimum are encountered around May, September and December. May and December are the months in which there is the registration of peaks for water, while September is linked with vegetation.

To this end, the last class to be analyzed is vegetation. As we can see this class corresponds to an important part of the pixels classified for each months. In Tab. 3 we

can see that the average values for vegetation corresponds to 41% of the pixels evaluated for all the years analyzed. This number seems to be impressively high, but anabranching rivers are characterized by the presence of generally stable vegetation on islands, that divide the flux into different branches (see subchapter 3.1.4). Thereby the average value is coherent with the definition for this morphology, hence we have another proof that our first classification has been done correctly. As a general information, in this case we can see a slight increment in stable vegetation in the 5 years, even though the seasonal peaks are the most outstanding trend. In fact if we have a look at Tab. 3 we can see that the average pixels classified as vegetated increments each year. In 2018 there is a value of 37% for vegetation class; it remains constant until 2020, and between 2021 and 2022 it reaches an impressive value of 50%. The increment is mainly at the expense of water that has a peak of 43% in 2018, while it decrease until reaching 29% in 2022. For what concerns the seasonal trends of vegetation figure a[1] is pretty representative and intuitive to read. If we have a look at it we can appreciate that there is a peak of vegetation around September, while the lowest vegetated area are found to be in wintertime around December-January.

A further step in the description can be done, in fact in December 2019, as we have already said, a flood event occurred. During floods, water carries sediment and deposit it in the active channel, when the flood wave pass. The sediment covers as a blanket morphology, and the vegetation that thrives above it. From a flooding event on, vegetation has to recolonize spaces that were taken from it. The 2019 episode allowed sediment to take over space respect to vegetation, but since such an event occurred just that year, vegetation had the capability to recolonize the environment. With an increase in vegetation class values there is a decrease in sediment class percentages. What satellite image classification in this case allow us to do, is to gain information on the recolonization of islands and bars by young plants, and therefore the creation of new habitats.

4.2.1.2 Transitional morphologies: temporal variations

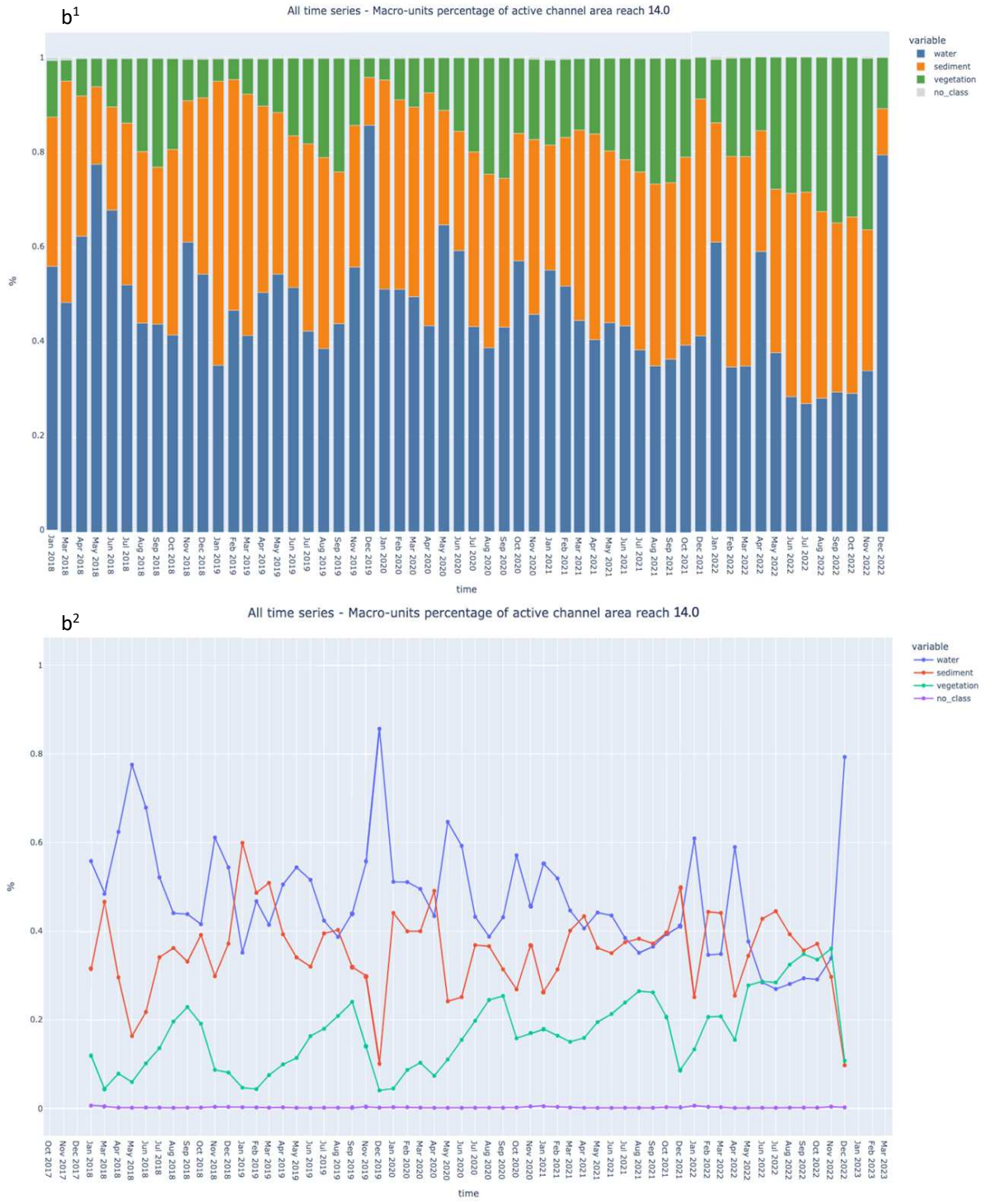

Fig. 23. *Trends from January 2018 to December 2022 of water, sediment and vegetation for reach 14; b1 bar plot; b2 lineplot.*

These plots represent the 5 years trend of reach 14 (Fig. 16 b.), that has been classified as transitional. Also in this case all the three classes will be described, starting from water going through sediment and finishing with vegetation.

In this reach water represent, the main class with values on average of 48% of the pixels classified. As for the previous reach, also here a general decrease of water values is encountered and is linked with the 2022 drought. The seasonal trends are consistent with reach 5 and follows the same path, reaching maximum peaks around December-January and May, and minimum around March-April and July-August. During December 2019 there is the highest peak reaching the impressive value of 86%, that corresponds to the flood event consistently with data of reach 5. Other two important peaks have been reached: one in May 2018, which is linked with a perturbation that interested North Italy for the whole month of May (Paolo Faggella, 2018), and the last peak reached in December 2022. About December 2022 there is a registration of a peak due to rainfall that went back to normality after the intense drought. For what concerns sediment class, here it has a more relevant role. This is because rivers tend to assume transitional morphologies where there is abundance of sediment to distribute. A relationship between water and sediment is more evident here than in reach 5. In correspondence with water peaks there is a low in sediment, that usually registers a huge increase the following month. After a high flow event usually sediment takes over vegetation's spaces and reshape the active channel. During summer vegetation grows and creates new habitats. The loops starts again when the first flooding event occurs.

In this frame of extreme dynamism of the morphology, it is important to collect more information on riparian vegetation to assess stability and the age of the bar surface (Carbonneau et al., 2020). In light of this, vegetation trends here are represented by a general increase from 2018 to 2022, with seasonal trends consistent to the one of reach 5. As a general observation the trend of decrease in water and increase in vegetation has been seen also in this reach, with a decrease from 56% of water class in 2018 to a 40% in 2022, and an increase from 12% to 25% for vegetation (Tab. 3).

4.2.1.3 Straight morphologies: temporal variations

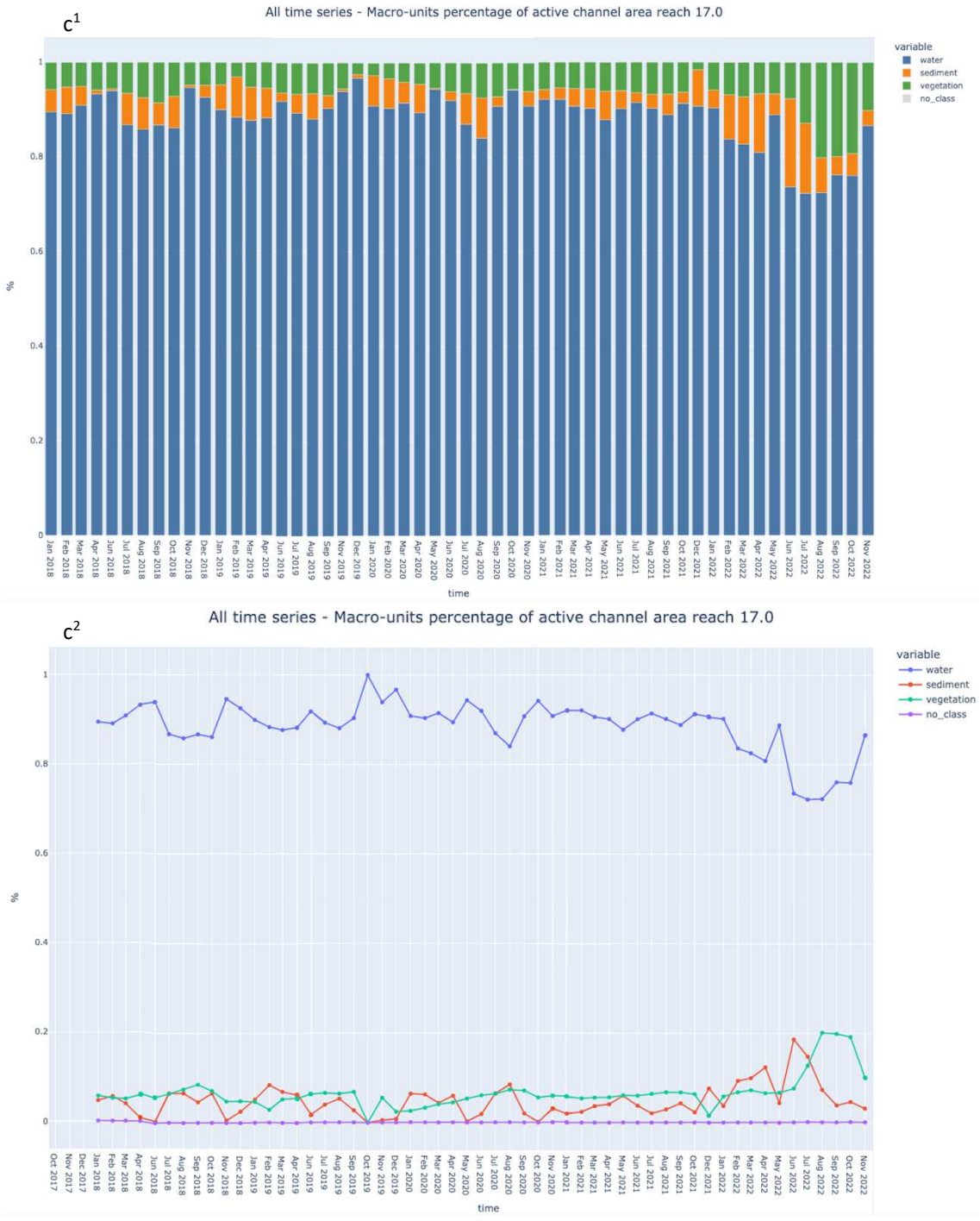

Fig. 24. *Trends from January 2018 to December 2022 of water, sediment and vegetation for reach 17; c1 bar plot; c2 lineplot.*

In this case plots are referring to a straight reach. As already mentioned, there are very few straight natural reaches. They are often associated with anthropic interference, in this case likely to be attributed to riverbanks modification and confinement of the riverbed (see subchapters 4.1 and 2.2.1).

From Fig. 24 c^2 is evident the shift between water and the other two classes. From the graphs in Fig. 23 there is a very outstanding difference, related to the sharp distinction among water and the rest. In fact water in this reach constitutes the dominant part with values around 90% of the total classified pixels. Differently from the previous reaches here the situation has been quite steady until 2021. It has just been influenced by the big drought of 2022, with a reduction of 8% of water in that year, and an increase in vegetation and sediment of 4% for both classes. Seasonal fluctuations here seems to be a little shifted compared to the previous reaches. Maximum peaks are registered around May-June and October-November, and minimum values are encountered during Summer months, and around February.

Sediment class behavior is the same as in reach 17 (Fig. 16 c.), while the increment in vegetation is less evident throw years, if compared with reach 5 and 14, even though is still quite impressive for 2022.

If we have a look at table 4 though, the increase in vegetation and in sediments for 2022 corresponds and is of 4% for both classes.

The same trend found in reach 5 and 14 of decrease and increase of sediment related to water is present also here.

For what concerns vegetation, the amount of variation between Summer and Winter is less visible. This can be linked to the stability of the reach, nevertheless the riparian vegetation fluctuations are characterized with a little peak during September.

4.2.1.4 Meandering morphologies: temporal variations

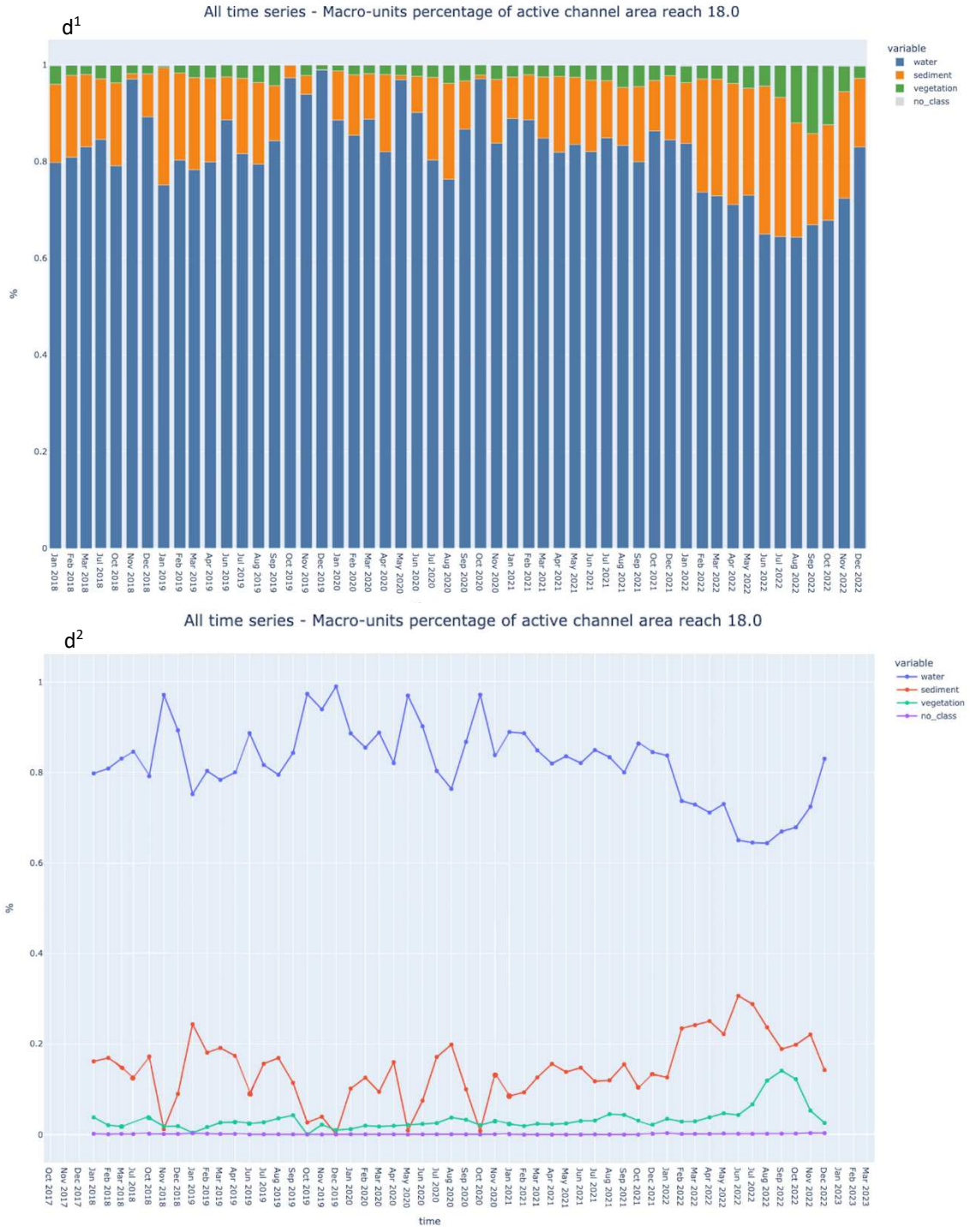

Fig. 25. *Trends from January 2018 to December 2022 of water, sediment and vegetation for reach 18; d1 bar plot; d2 lineplot.*

This plots analyze the changes throughout 5 years of the three semantic classes for the meandering reach number 18 (Fig. 16 d.).

Also in this case there is an evident separation between water and the other classes, as in reach 17. The majority of pixels have been classified as water, with an average value of 83% (Tab. 3).

Water trends follow what has been seen in all the other reaches, with a general decrease in values from 85% registered in 2018 to 72% in 2022.

Seasonal trends are characterized by two peaks: one in October and the other in May, and a less pronounced peak around December. The variation of water around peaks is minimal, but more evident compared to the straight reach, with a variation of about 15% on average.

Sediment has a quite impressive role compared to vegetation; pixels classified as sediment correspond on average, to 14% while vegetation accounts just for 3%.

During peaks of water sediment reach its lowest value, as expected, while a decrease in vegetation is not registered. Maybe this can be linked to the presence of a more stable vegetation in the active channel, that is less affected by water, therefore sediment, fluctuations. Moreover, if we have a look at Fig. 25, is evident that this reach appears to be very constricted by croplands, therefore riparian vegetation doesn't have much space to grow along the reach.

Usually vegetation and sediment go hand in hand, with the increase of one class there is the decrease in the other. Here this trend is basically nonexistent until 2022, where with a decrease in water during the first month, we have an increase in sediment, followed the next months by the increase in vegetation.

The seasonal trend for vegetation can be recognized also here, even though the variations are very low around 3% until 2022, when the increase has been of 10%

4.2.1.5 Sinuous morphologies: temporal variations

Fig. 26. *Trends from January 2018 to December 2022 of water, sediment and vegetation for reach 24* (24*= reach 24 and 25, for the sake of simplicity from now on it will be mentioned just as reach 24*); e1 bar plot; e2 lineplot.*

This plot characterize sinuous morphology. Here are presented the trend found in reach 24*, that has both been classified as sinuous.

As for figures 24 and 25, also in this case, the predominant class is represented by water (89% on average – Tab. 3).

Here as well, the trends for this class are the same as in the previous plots analyzed, with a general decrease through the 5 years, and a seasonality with positive peaks in Spring and Winter, and negative peaks during Summer months.

A change compared to previous reaches' trends, here is that during March 2018 an impressive minimum in water occurred and is pretty evident by looking at Fig. 26 e^2. During this month there has been a decrease of around 30% of water.

This reach is located downstream of Serafini Island (Fig. 21.), where, as already said, a dam is located. Moreover in 2012 new works began, the aim of which has been to build a new navigation channel (AIPo, 2018). In March 2018 it has been opened, the same month a minimum in water has been registered on the reach (Fig. 26). The fact that this trough is found just in this reach, and that it appears to occur the same month as the opening of the navigation channel, might suggest a correlation between the two.

This hypothesis has to be confirmed though, by a more extensive study, and doesn't fall into the core theme aim of this dissertation.

Sediment and vegetation here are similar to reach 17, with overlapping lines (Fig. 26 e^2). Sediments have an inverse relation with water when one increases the other decreases, no other particular trends are evidenced.

On the other hand vegetation behaves differently from other reaches, it is still interested by an increase throughout the 5 years, but it is very little. Even though the fluctuations are barely evident, the seasonal trend is still recognizable.

	Reach 5 anabranching			Reach 14 transitional			Reach 17 straight			Reach 18 menadering			Reach 24* sinuous		
	W	S	V	W	S	V	W	S	V	W	S	V	W	S	V
2018*	0,43	0,20	0,37	0,56	0,32	0,12	0,90	0,04	0,06	0,85	0,12	0,03	0,88	0,07	0,04
2019*	0,35	0,25	0,39	0,50	0,38	0,12	0,91	0,04	0,05	0,85	0,13	0,02	0,89	0,07	0,04
2020*	0,32	0,26	0,37	0,50	0,36	0,15	0,90	0,04	0,05	0,87	0,11	0,02	0,90	0,06	0,04
2021*	0,32	0,24	0,44	0,43	0,38	0,19	0,90	0,04	0,06	0,85	0,13	0,03	0,91	0,05	0,04
2022	0,29	0,22	0,50	0,40	0,34	0,25	0,82	0,08	0,10	0,72	0,22	0,06	0,87	0,07	0,06
Total average	0,34	0,23	0,41	0,48	0,36	0,17	0,89	0,05	0,07	0,83	0,14	0,03	0,89	0,06	0,05
Indexes values	**Si**	**Bi**	**Ai**	**Si**	**Bi**	**Ai**	**Si**	**Bi**	**Ai**	**Si**	**Bi**	**Ai**	**Si***	**Bi***	**Ai***
	1,07	1,21	1,57	1,08	1,46	1,16	1,02	1,07	1,07	2,08	1,04	1,07	1,24	1	1,14

Tab. 3. *In the upper part are presented the averages for each of the semantic classes (W= water, S= sediment, V= vegetation) for the years analyzed. The averages from 2018 to 2021, that are followed by * symbol, have been calculated excluding the months that didn't had available data for that reach. For what concerns indexes (see chapter 3.1.3) the only modification that has been performed is relative to reach 24*, for which has been reported an average value based on the original values of both the reaches.*

4.2.1.6 Comparison among all the reaches, for all the semantic categories

In this section a comparison among water, sediment and vegetation classes will be done, in order to understand if there are remarkable variations in the response of pixels for different morphologies. Is important to point out that a high value in percentage doesn't represent that there is more of that feature in a reach, but that the distribution of morphological units (water, sediment and vegetation) create different configurations. This analysis is a representation of the process that lead to the formation of a morphological pattern instead of another. Basically what has been done in the following part is the analysis of how a morphology of a reach is characterized in terms of morphological units distribution and their associated dynamics over time.

The three graphs in Fig. 25 have on the x axes, the time, while on the y axes each of them have one of the three classes.

- Water: Fig. 25 a. presents the trends of water for the five morphologies analyzed. As we can see straight, sinuous and meandering reaches are characterized by very high percentages of water, while anabranching and transitional reaches have, on average, less pixels in the water class.

  Negative peaks in general are seen for all the reaches around March and August and corresponds to the observations found in previous subchapters. The same can be applied for positive peaks, found around May and December.
- Sediment: Fig 25 b. represents the trends of sediments. In this case there is the opposite situation from graph a. In fact, what is evident is that transitional reaches are characterized by much more sediment than other morphologies. This is coherent with the definition of transitional reach and is a further proof that it has been well classified. The second most rich morphology is anabranching, and also in this case, it sticks with the definition. The morphology with least percentage of sediment is straight. This lack of material is probably due to the conditions of the reach, which is

strongly anthropized and confined, and therefore channel incision is probably the predominant process (see subchapter 2.2.1.2)

For what concerns seasonal variations, positive peaks in the values are reached around winter season and in summer. Negative peaks on the other hand are registered to be around May and August, one corresponds with a peak in precipitations, therefore water, the other with a peak in vegetation expansion.

- The last class is vegetation, that is presented in Fig. 25 c. The seasonal trend is extremely evident, and for the morphology with a huge abundance in vegetation the variation is impressive, with variations close to 30%. The anabranching reach, has the highest values (see subchapter 4.2.1.1), followed by the transitional reach. The other morphologies are quite overlapping in values, even though straight reach seems to have more vegetation than sinuous and meandering reaches. What appears clearly is the intensity of variation. For anabranching and transitional reaches, the variation can reach up to 30%, while for the other morphologies it reaches a peak of 15% during 2022, the year of the drought.

  Overall the positive peaks are registered to be between August and September, while the negative are around winter between December and February. For this class the variations are less abrupt because vegetation needs time to grow and is a continuous process.

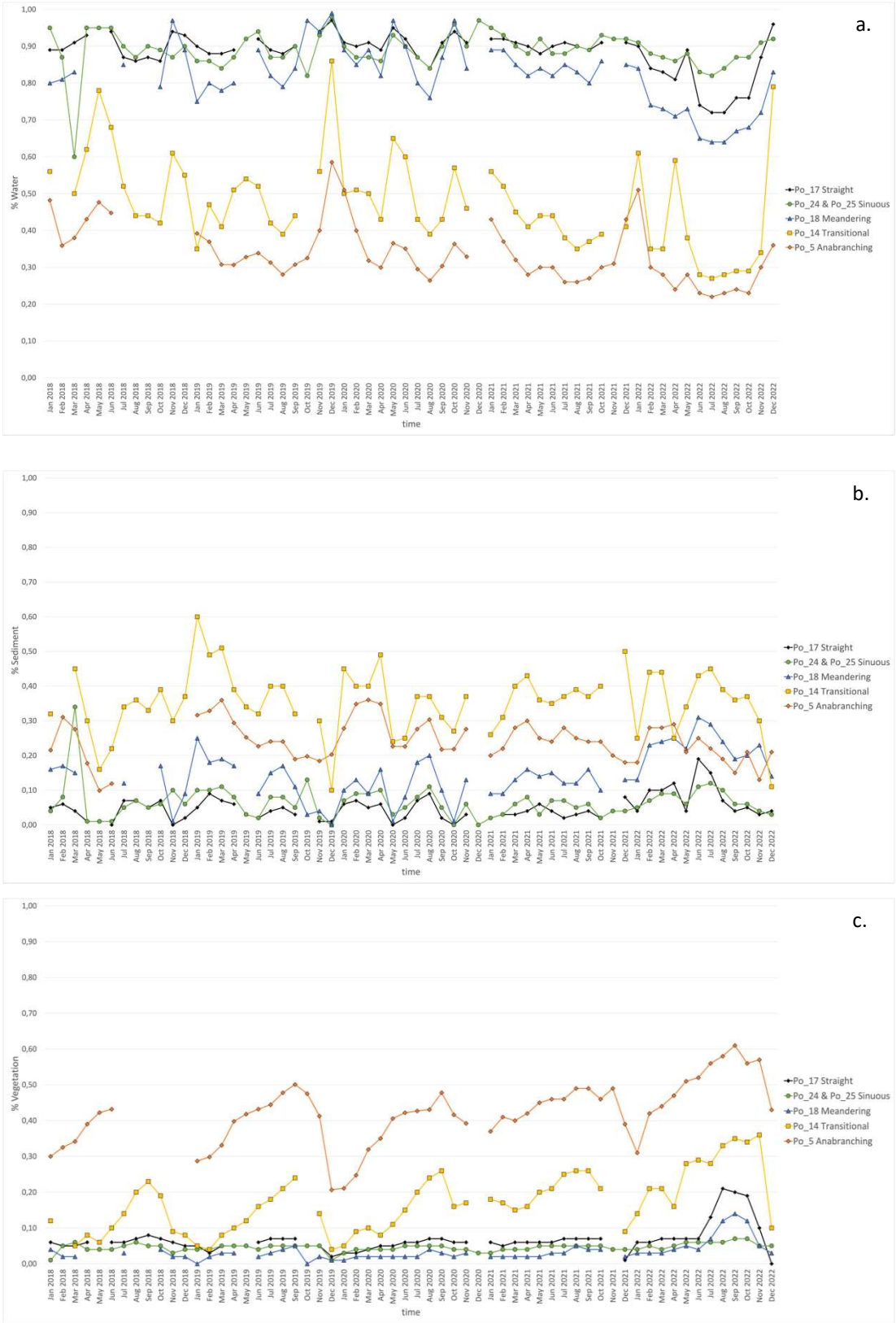

Fig. 27. *In all the graphs on the x axe there is time, while on the y axe there is the percentage value of a class. All the morphologies of reaches are compared to each other for the three semantic classes; a. water %; b. sediment %; c. vegetation%.*

If we have a look at Fig. 28, there is the comparison between percentages in water and sediments for all the morphologies. The morphologies can be divided into two main groups. One that comprehends anabranching and transitional patterns, and the other that contains meandering, sinuous and straight patterns.

The first group is characterized by the presence of more sediment than water. This observation is coherent with W* (Fig. 19) and the sediment supply. In fact, for the same drained area, generally transitional and anabranching reaches have more sediment than straight, sinuous and meandering.

The second group, composed of straight, meandering and sinuous patterns, is characterized by higher percentages of water and less sediment. This trend represents the conditions of a single, deep channel with a narrow section. In this case W* will be little if compare with the first group's morphologies, and in fact these patterns forms when less sediment has to be accommodated, for the same drained area.

The very little amount of sediment can be linked also with anthropic interventions. If a reach with high percentages of sediment is mined, it will take less time to recover if compared to a reach that has less sediment supply. Therefore the buffering time will be different, and this graph may represent it. Moreover single channel reaches tend to be confined more impacted by engineering interventions, because the channel course is more stable if compared to other patterns (e.g. transitional). As seen in chapter 2.3.2 confinement enhance the channel incision phenomenon. A proof of this occurrence is that the straight reach is characterized by high amount of water and very few sediments. Straight reaches are unnatural, and usually a direct consequence of anthropic interventions. To find them on the right side of graph in Fig. 28 gives us a hint on anthropic intervention, that can be applied also for meandering and sinuous morphologies.

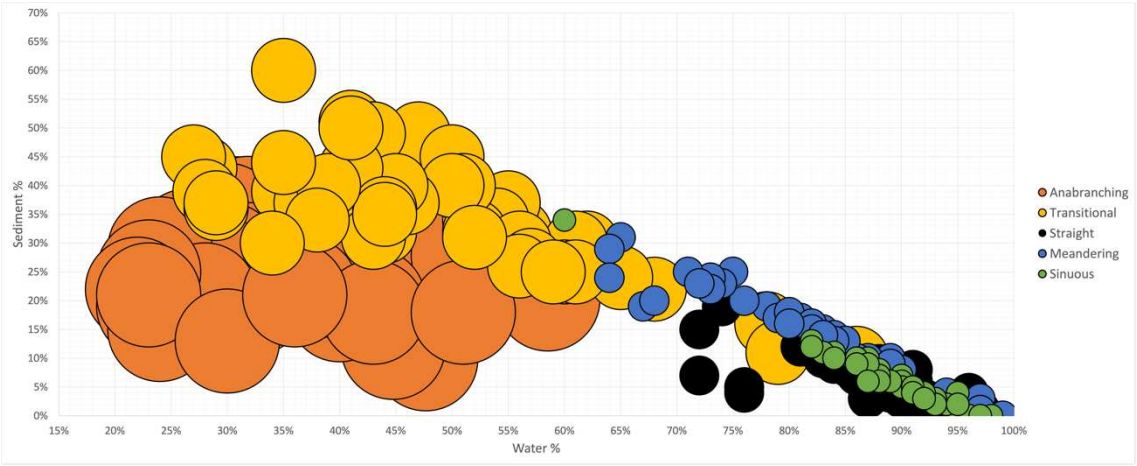

Fig. 28. *Plot of sediment % vs. water %, the dimension of points is given by the value of W*. Patterns can be divided into two main groups, one characterized by a lot of sediment respect to water, and the other with more water than sediment. The first group comprehends anabranching and transitional morphologies, that, in fact have to accommodate more sediment than the other three patterns, for the same drained area. On the other hand the second group is characterized by patterns that have much more water than sediment in the active channel. Therefore W* will be little if compared with the first group's members.*

5. Conclusions

The aim of this thesis has been to compare traditional geomorphological classification of rivers, and a new classification based on Sentinel-2 images.

Until now satellite images-derived data has been used mainly to verify knowledge, instead of creating new understanding of natural processes (Piégay et al., 2020). This thesis has tried to understand which new information can be obtained by the implementation of new tools, on river geomorphology.

The comparison of two methods has been done on Po River, which is the longest river in Italy. It has been chosen due to its incredibly morphological variety, that comprises various river patterns (Tab 1).

Firstly a traditional classification has been performed, based on the IDRAIM handbook (Rinaldi et al., 2014). This type of classification utilized orthophotos of sub-meter spatial resolution, in the order of centimeters. On the other hand it lack temporal resolution, in fact the acquisition of orthophoto happens once every 5 to 10 years.

The first step has been to perform the analysis of orthophotos, and high-resolution satellite images, from which characterizing indexes (anabranching, braiding and sinuosity) has been calculated. The second step has been to identify parts of the river that are characterized by a similar morphology, and therefore that can constitute a fundamental morphological unit called reach (Brenna et al., 2022). A final step has been performed, with the calculation of both slope (%) and W* (normalized drainage area – Fig. 15; Fig. 17).

W* has not been used in this river-geomorphological classifications, but still provides valuable information to distinguish different morphology (Piégay et al., 2009). Patterns that have to accommodate more sediment are characterized by a higher value in W* (Liébault et al., 2013) and are found in more steep areas and are characterize by multiple channels pattern. Reaches that need to accommodate less sediment are characterized by smaller values for slope and single channel pattern.

The second classification performed has been based on Sentinel-2 images, which are characterized by a very high time resolution, with a recurrency of the acquisition on the

same part of the world of about 5 days, but less spatial resolution (around 10 meters - ESA, 2015). The baseline has been still the traditional classification, from which the most representative reaches for each morphology has been chosen.

The first step has been to download all the images for each reach from 2018 to 2022. For each of the images the fuzzy classification created by Carbonneau et al. (2020) has been performed (Fig. 14). It assigns, to each pixel of the image, a percentage value in one of the three classes taken into consideration which are: water, sediment and vegetation. A further step has been done; based on the fuzzy classifications, exploiting a code wrote in python by Micotti M. and modified by Bozzolan E., graphs that represents trends for the three classes throughout the 5 years, for each river reach, have been created (Figures 22,23,24,25,26).

What emerges from this analysis and comparison is interesting. Traditional classification provides a very detailed representation of a river in a precise moment of its evolution, with a detail that goes down to centimetric resolution. Thanks to this analysis a state-of-the-art for a certain river in a certain moment is provided.

What emerges from the traditional classification on Po River, is that the passage from one morphology to another, even though is determined by sharp boundaries, is more continuous. To go from a pattern to another the transition has all the intermediate possible configurations, before trespassing the sharp threshold (Gurnell et al., 2009).

With the calculation of slope and W* this gradual distinction emerges (Fig. 19), and a further observation can be done. In fact reaches with more sediment, such as anabranching and transitional, are usually characterized by higher slopes and higher values in the normalized drainage area. On the other hand reaches characterized by a single channel, are found in less steep areas and with a little value for W*.

It is interesting then to analyze the dynamic of geomorphic units with multiple images per month from 2018 to 2022 for each of the classified morphology by satellite-images classifications.

Indeed satellite-images classification can give us a hint on the processes that are occurring in each reach, because information are frequent in time.

The first consideration is linked with water, for all the reaches a decrease in the percentage values form 2018 to 2022, for this class has been registered. The trough corresponds with the extreme drought that hit Italy on 2022, with a decrease of about 10% of water for all the reaches.

Moreover in all the graphs (Fig. 22,23,24,25,26) has been possible to see seasonal variations in all the three classes. The most evident seasonal trend has been found for riparian vegetation, that has a low during winter season, than starts to grow until reaching a peak around August-September. Another interesting factor that rise from this classification is the relation between floods and vegetation. In particular what have been seen is that in winter 2019 a flood event occurred; water carried sediment that covered everything in the active channel, burying vegetation. Vegetation took time to regrow, but stabilized within a short time, restoring and creating new habitats almost entirely before the following winter. This observations might be very useful to control renaturation and restoration projects. In a first broad analysis the areas can be evaluated by looking at graphs such as Fig. 22, but to confirm that the renaturation has been achieved, a ground truth is fundamental.

Another important trend can be found comparing water and sediment percentages for the different morphological patterns (Fig. 28). What emerges is that there is a straight correlation between water and sediment. Anabranching and transitional morphologies are characterized by a higher pixels classified as sediment, and less water. In fact these two patterns have to accommodate more sediment for the same drained area (W*) if compared to other morphologies. This trend has been recognized also with a more transitional classification but is very evident with satellite-images derived data analysis. Also in this case, single channel morphologies are characterized by a strong presence of water rather than sediment. This might be due to anthropic interventions that are more incisive for reaches where the amount of sediment is less, probably because the

buffering time to adjust to riverbed mining and confinement takes more time than for sediment-rich patterns (Surian & Rinaldi, 2003).

In general satellite-images classifications are a very powerful tool, that can enrich traditional classification, by providing new hints on the processes occurring, thanks to the very frequent acquisitions in time (Carbonneau & Piegay, 2012). The tool is very powerful for medium-large river (wider than 50m, headwaters are neglected) and if used continuously will provide information on river dynamics, helping with the development of more accurate previsions for future changes. In this case it helped with the establishment of a general decrease of water in the Po river, and with the observation of more seasonal phenomena (Bozzolan Elisa et al., 2023 - under revision).

As last point is important to mention that satellite-image classifications are cost-effective, because don't require the implementation of specific instrumentation, but are based on data that are acquired anyway, regardless of the use.

On the other hand traditional classification remains the baseline to start from, to identify river reach on which clip satellite classification and analyze their data. Although such approach portraits the situation in a specific moment, it does it with high resolution in terms of mapping river feature details.

Both of the classifications are meaningful to be used, and integrated. IDRAIM and similar applications (Fryirs & Brierley, 2013) characterize the river morphology in details and defines reaches and patterns, satellites derived mapping can support the quantification of geomorphic units dynamics within each reach and then provide monitor and predicting abilities to foresee river geomorphological trajectories. This is a precious information to support modern river management which can applied globally on common metrics and data.

References

AdbPo. (2008). *Il recupero morfologico ed ambientale del fiume Po*. Diabasis.

AdbPo. (2022). *Rinaturazione dell'area del Po, PNRR M2C4 investimento 3.3 Programma d'Azione*.

AIPo. (2018). *23 marzo 2018, inaugurazione della nuova conca di navigazione di Isola Serafini (PC)*. agenziapo.it. https://www.agenziapo.it/content/23-marzo-2018-inaugurazione-della-nuova-conca-di-navigazione-di-isola-serafini-pc

Alber, A., & Piégay, H. (2011). Spatial disaggregation and aggregation procedures for characterizing fluvial features at the network-scale: Application to the Rhône basin (France). *Geomorphology*, *125*(3), 343–360. https://doi.org/10.1016/j.geomorph.2010.09.009

Andrea Colombo. (2022, November 16). *Un programma d'azione che viene da lontano*. Processo informativo e partecipativo relativo al Programma d'azione del Progetto «Rinaturazione dell'area del Po».

Bocchino, F., Ravanelli, R., Belloni, V., Mazzucchelli, P., & Crespi, M. (2023). WATER RESERVOIRS MONITORING THROUGH GOOGLE EARTH ENGINE: APPLICATION TO SENTINEL AND LANDSAT IMAGERY. *The International Archives of the Photogrammetry, Remote Sensing and Spatial Information Sciences*, *XLVIII-M-1–2023*, 41–47. https://doi.org/10.5194/isprs-archives-XLVIII-M-1-2023-41-2023

Boothroyd, R. J., Williams, R. D., Hoey, T. B., Barrett, B., & Prasojo, O. A. (2021). Applications of Google Earth Engine in fluvial geomorphology for detecting river channel change. *WIREs Water*, *8*(1). https://doi.org/10.1002/wat2.1496
Bozzolan Elisa, Brenna Andra, Surian Nicola, Carbonneau Patrice, & Bizzi Simone. (2023). *Quantifying the impact of the spatiotemporal resolution of the Sentinel 2 images on the interpretation of the active channel trajectory. An application on a dynamic river reachsection in Northern Italy.*

Bravard, J.-P., Landon, N., Peiry, J.-L., & Piégay, H. (1999). Principles of engineering geomorphology for managing channel erosion and bedload transport, examples from French rivers. *Geomorphology*, *31*(1–4), 291–311. https://doi.org/10.1016/S0169-555X(99)00091-4

Brenna, A., Bizzi, S., & Surian, N. (2022). A width-based approach to estimating historical changes in coarse sediment fluxes at river reach and network scales. *Earth Surface Processes and Landforms*, *47*(10), 2560–2579. https://doi.org/10.1002/esp.5395

Brice J.C. (1975). *Air photo interpretation of the form and behaviour of alluvial rivers.Final report to the US Army Research Office.* (AD-A008 108). Army research office. https://apps.dtic.mil/sti/pdfs/ADA008108.pdf

Carbonneau, P. E., Belletti, B., Micotti, M., Lastoria, B., Casaioli, M., Mariani, S., Marchetti, G., & Bizzi, S. (2020). UAV-based training for fully fuzzy classification of Sentinel-2 fluvial scenes. *Earth Surface Processes and Landforms*, *45*(13), 3120–3140. https://doi.org/10.1002/esp.4955

Carbonneau, P. E., & Piegay, H. (2012). *Fluvial Remote Sensing for Science and Management*.

Chi, M., Plaza, A., Benediktsson, J. A., Sun, Z., Shen, J., & Zhu, Y. (2016). Big Data for Remote Sensing: Challenges and Opportunities. *Proceedings of the IEEE*, *104*(11), 2207–2219. https://doi.org/10.1109/JPROC.2016.2598228
ESA. (2015). *SENTINEL-2 MISSION GUIDE*. Sentinel.Esa.Int. https://sentinel.esa.int/web/sentinel/missions/sentinel-2

Fryirs, K. A., & Brierley, G. J. (2013). *Geomorphic analysis of river systems: An approach to reading the landscape* (1. publ). Wiley-Blackwell.
Gurnell, A., Surian, N., & Zanoni, L. (2009). Multi-thread river channels: A perspective on changing European alpine river systems. *Aquatic Sciences*, *71*(3), 253–265. https://doi.org/10.1007/s00027-009-9186-2

Jean-René Malavoi & Jean-Paul Bravard. (2010). *Eléments d'hydromorphologie fluviale*. ONEMA.

Kondolf, G. M., & Piégay, H. (Eds.). (2016). *Tools in fluvial geomorphology* (Second edition). John Wiley & Sons.

Leopold L.B. & Wolman M.G. (1957). *River channel patterns: Braided, meandering, and straight* (Professional Paper) [Professional Paper].

Liébault, F., Lallias-Tacon, S., Cassel, M., & Talaska, N. (2013). LONG PROFILE RESPONSES OF ALPINE BRAIDED RIVERS IN SE FRANCE: LONG PROFILE RESPONSES OF ALPINE BRAIDED RIVERS IN SE FRANCE. *River Research and Applications*, *29*(10), 1253–1266. https://doi.org/10.1002/rra.2615

Marcus, W. A., & Fonstad, M. A. (2010). Remote sensing of rivers: The emergence of a subdiscipline in the river sciences. *Earth Surface Processes and Landforms*, *35*(15), 1867–1872. https://doi.org/10.1002/esp.2094

Montanari, A. (2012). Hydrology of the Po River: Looking for changing patterns in river discharge. *Hydrology and Earth System Sciences*, *16*(10), 3739–3747. https://doi.org/10.5194/hess-16-3739-2012

Paolo Faggella. (2018). *Maggio 2018: Precipitazioni eccezionali per abbondanza e frequenza*. https://datimeteoasti.it/articoli-analisi-climatiche/maggio-2018-piogge-eccezionali-abbondanza-frequenza/

Parrinello, G. (2018). Systems of Power: A Spatial Envirotechnical Approach to Water Power and Industrialization in the Po Valley of Italy, ca.1880–1970. *Technology and Culture*, *59*(3), 652–688. https://doi.org/10.1353/tech.2018.0062

Parrinello, G., Bizzi, S., & Surian, N. (2021). The retreat of the delta: A geomorphological history of the Po river basin during the twentieth century. *Water History*, *13*(1), 117–136. https://doi.org/10.1007/s12685-021-00279-3

Piégay, H., Alber, A., Slater, L., & Bourdin, L. (2009). Census and typology of braided rivers in the French Alps. *Aquatic Sciences*, *71*(3), 371–388. https://doi.org/10.1007/s00027-009-9220-4

Piégay, H., Arnaud, F., Belletti, B., Bertrand, M., Bizzi, S., Carbonneau, P., Dufour, S., Liébault, F., Ruiz-Villanueva, V., & Slater, L. (2020). Remotely sensed rivers in the Anthropocene: State of the art and prospects. *Earth Surface Processes and Landforms*, *45*(1), 157–188. https://doi.org/10.1002/esp.4787

Ramapriyan, H. (2013, October 18). *Managing Big Data*. Eijournal.Com. https://eijournal.com/print/articles/managing-big-data

Riccardi Giuseppe & Comune Elisa. (2019). *Evento piena Po novembre 2019* (p. 16). Arpae.

Rinaldi M., Braca G., Bussettini M., Gurnell A.M., García de Jalón D., González del Tánago M., Lastoria B., Martínez-Fernández V., Mosselman E., & Percopo C. (2015). *REFORM REstoring rivers FOR effective catchment Management Methods, models, tools to assess the hydromorphology of rivers—Part 2 Thematic Annexes on monitoring indicators and models*. https://www.reformrivers.eu/system/files/6.2%20Methods%20to%20assess%20hydromorphology%20of%20rivers%20part%20II.pdf

Rinaldi, M., Gurnell, A. M., Del Tánago, M. G., Bussettini, M., & Hendriks, D. (2016). Classification of river morphology and hydrology to support management and restoration. *Aquatic Sciences*, *78*(1), 17–33. https://doi.org/10.1007/s00027-015-0438-z

Rinaldi, M., Surian, N., Comiti, F., & Bussettini, M. (2014). *IDRAIM – Sistema di valutazione idromorfologica, analisi e monitoraggio dei corsi d'acqua ISPRA*. ISPRA. https://www.isprambiente.gov.it/it/pubblicazioni/manuali-e-linee-guida/MLG113_2014_IDRAIM_rev_settembre2015ridotto.pdf

Rinaldi, M., Surian, N., Comiti, F., & Bussettini, M. (2015). A methodological framework for hydromorphological assessment, analysis and monitoring (IDRAIM) aimed at promoting integrated river management. *Geomorphology*, *251*, 122–136. https://doi.org/10.1016/j.geomorph.2015.05.010

River restoration in Europe: Practical approaches. (2001). Institute for Inland Water Management and Waste Water Treatment.

Roux, C., Alber, A., Bertrand, M., Vaudor, L., & Piégay, H. (2015). "FluvialCorridor": A new ArcGIS toolbox package for multiscale riverscape exploration. *Geomorphology*, *242*, 29–37. https://doi.org/10.1016/j.geomorph.2014.04.018

Surian, N., & Rinaldi, M. (2003). Morphological response to river engineering and management in alluvial channels in Italy. *Geomorphology*, *50*(4), 307–326. https://doi.org/10.1016/S0169-555X(02)00219-2

UCAR. (2023). *Network Common Data Form (NetCDF)*. Unidata.Ucar.Edu. https://www.unidata.ucar.edu/software/netcdf/